Peer-reviewed version available at *Quaternary* **2018**, *1*, 14; doi:10.3390/quat1020014

Article

Specifying the External Impact on Fluvial Lowland Evolution: the Last Glacial Tis(Z)a Catchment In Hungary and Serbia.

Jef Vandenberghe[1], Cornelis (Kees) Kasse[1], Dragan Popov.[2], Slobodan Markovic, [2], Dimitri Vandenberghe[3], Sjoerd Bohncke[1†] and Gyula Gabris[4]
[1] Department of Earth Sciences, Vrije Universiteit, De Boelelaan 1085, 1081HV Amsterdam, The Netherlands; jef.vandenberghe@vu.nl
†deceased
[2] Department of Geography, Tourism and Hotel Management, Faculty of Science, University of Novi Sad Trg Dositeja Obradovica 3, Novi Sad 21000, Serbia; baca.markovic@gmail.com
[3] Laboratory of Mineralogy and Petrology, Department of Geology, Ghent University, Krijgslaan 281 (S8), B-9000 Gent, Belgium; davdenbe@gmail.com
[4] Department of Physical Geography, Eötvös University of Budapest, H-1117 Budapest, Pázmány st. 1/C, Hungary; ferencgyula@caesar.elte.hu
*correspondence: jef.vandenberghe@vu.nl

Abstract
External impact on the development of fluvial systems is generally exerted by changes in sea level, climate and tectonic movements. In this study it is shown that regional to local differentiation of fluvial response may be caused by semi-direct effects of climate change and tectonic movement, as for instance vegetation cover, frozen soil, snow cover and longitudinal gradient. Such semi-direct effects may be responsible for specific fluvial activity resulting in proper drainage patterns, sedimentation series and erosion-accumulation rates. These conclusions are exemplified by the study of the Tis(z)a catchment in the Pannonian Basin in Hungary and Serbia from the middle of the last glacial to the Pleistocene-Holocene transition. Previous investigations in that catchment are supplemented here by new geomorphological-sedimentological data and OSL-dating. Specific characteristics of this catchment in comparison with other regions are the preponderance of meandering systems during the last glacial and the presence of very large meanders in given time intervals.

Keywords: Tisza, Tisa, Pannonian Basin, fluvial evolution, terrace development, tectonic impact, local conditions, last glacial, OSL-dating

1. Introduction

The impact of climate on fluvial activity and subsequent drainage patterns is recognized since a long time [1-3] in addition to other external forcing factors as tectonic movements, base-level changes and anthropogenic activity. Traditional correspondence between glacial-interglacial cycles and fluvial evolution has been modified since a few decades, focusing rather on the important fluvial morphological changes occurring at climate transitions, originally in temperate to periglacial environments by [4,5] and [6], later on slightly adapted by the same and other authors [7-9] and confirmed by many field cases (e.g. [10] and references therein). Meanwhile it has also been recognized in other climatic zones as the monsoonal environment, for instance in China [11, 12] and Australia [13]. It has been called a model of non-linearity as the fluvial action is influenced by the delayed effect of vegetation development with regard to the involved climatic change.

However, progressive fluvial research has demonstrated that the general validity of the, climatically driven, non-linear fluvial model may also need some adaptations in specific climate circumstances, e.g. in glacial [14-16] and arctic environments [17-18], Mediterranean environments [19, 20] and tropical conditions [21]. Often the external variables, climate and

tectonic movements, may play an indirect role. Such semi-direct climate influences are, e.g., the development of specific vegetation cover, the degradation of thick snow covers and glacier ice or the presence of frozen ground. Similarly, climate may have a direct impact on the power supply by the water flow characteristics that determine the discharge, but also indirectly on the sediment delivery to the drainage system (by the vegetation). Also the morpho-structural framework and topography, as indirectly imposed by the tectonic setting, give a characteristic identity to the catchment [22, 23, 15-16]. Especially the energy of the fluvial system is determined by the river gradient, which consequently represents a most influential factor in the eroding or accumulating character of a river. In addition, several studies consider the complexity of climate cycles with weakly expressed interstadials or stadials [24-25] or climatic episodes of short duration that hindered rivers crossing thresholds [26-28]. Finally, the ultimate morphological result of river action is determined by the preservation potential as an expression of the river's intrinsic evolution [26, 9, 29].

The present study concerns the Tisza catchment in the Pannonian (Carpathian) basin of Hungary and Serbia ('Tisa' in Serbian, Romanian and Ukrainian; 'Tisza' in Hungarian). Some years ago, first results were published by [30] for the middle Tisza in Hungary and by [31] for the lower Tisa in Serbia. Now we compare and extend that research in an adjacent area to the north in the middle Tisza and further downstream in the lower Tisa. This paper aims to illustrate the effects of a specific climatic and topographical setting on fluvial morphological development, namely that of temperate continental climate conditions in contrast to previous studies which generally dealt with more oceanic conditions. In addition, a low-relief, and thus low-energy topography is considered. It means, with regard to vegetation cover, that a more steppic environment rather than tundra is involved and, with regard to topography, that a low bedload-suspension load ratio is characteristic for this catchment due to its low gradient (Figure 1).

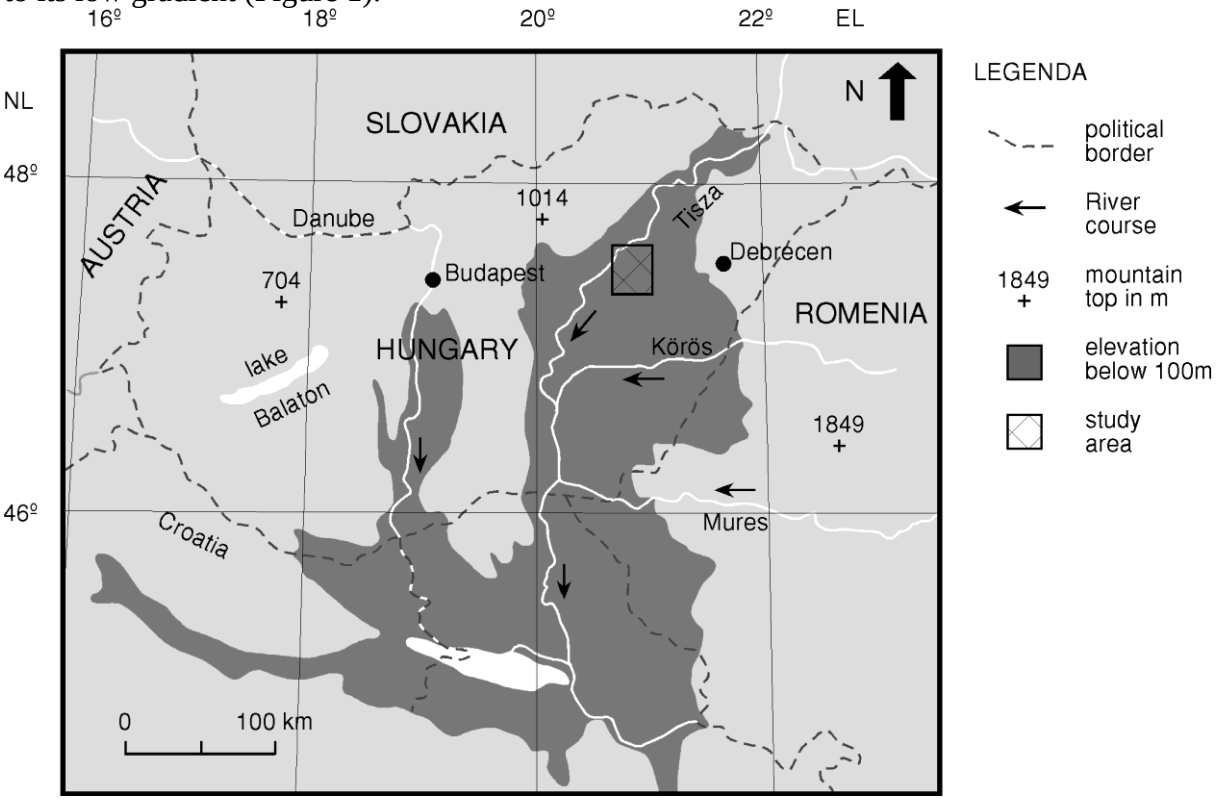

Figure 1 Location map of the Tis(z)a catchment in Hungary and Serbia.

2. Study region and previous research:

Peer-reviewed version available at Quaternary 2018, 1, 14; doi:10.3390/quat1020014

The Tis(z)a is a main tributary of the Danube, starting its course from the Eastern Carpathian Mountains in Romania, flowing through Ukraine to arrive in the Pannonian Basin in Hungary (middle Tisza) and finally in Serbia (lower Tisa), which is the lowest part of the Basin [32,33]. Both Danube and Tis(z)a formed their valleys in thick Quaternary basin deposits. Their wide floodplain shows an intriguing pattern of successive meandering systems and impressive fluvial deposits from the last glacial and Holocene, extensively described by [30, 34-36].

In comparison with the more northern periglacial-temperate regions, the environmental setting in the loess-covered Tisza catchment differed in a few aspects during the late Weichselian. Firstly, the vegetation cover was less dramatically reduced; probably a steppic cover including some tree refugia persisted in contrast to the bare tundra landscape in the northern coversand regions [37-38]. Secondly, the climate was more continental with colder winters, warmer summers and less precipitation [39]. Thirdly, the study region occurred in the marginal zone of permafrost at the end of the last glacial, in contrast to NW Europe that occurred distinctly within the permafrost belt [40-41].

Structurally, the Tisza catchment occurs in the Pannonian basin, a zone of considerable tectonic subsidence [42-44]. On the average the longitudinal gradients in the drainage system of the tectonic basin are very low, from c. 1,86 cm/km in the lower Tisa, 5-10 cm/km in SE Hungary to 15 cm/km in central-north Hungary, leading to almost purely suspension transport nowadays [30,31,35]. The evolution of the drainage system was obviously determined by the peculiar tectonic subsidence pattern during the Pleistocene. In addition, this tectonic impact was superseded by evident climatic imprints [30, 35,36, 45-47].

3. Methods

Following the original research set-up applied by [30], information on the sedimentary architecture was acquired by topographic (DEM) analysis and field investigations mainly consisting of transects across the present floodplain using hand-drill data and a few geoelectric sections. Detailed coring enabled to reconstruct the precise geometry of former, now abandoned channels. A semi-closed gouge and suction-tube corer were used in the water-saturated sediments. Drill coring was supplemented with exposure data from sand or clay exploitation pits. Apart from palynological analyses [30], sedimentological analysis involved grain-size measurements by laser diffraction [48]. The latter paper describes in detail the preparation method of the grain-size analyses involving, for instance, removal of calcium carbonate and organic material by adding HCl and H_2O_2, respectively, and, amongst others, initiated the clay-silt boundary at 8 µm which we apply here.

Our previous work in the Tisza basin demonstrated the complexity of interpreting chronologies derived from radiocarbon dating for reason of possible and uncertain degree of reworking [30]. The present project therefore explores the possibilities of luminescence dating. Luminescence research in the Hungarian fluvial domain has been summarised by [36]. First results in the Serbian domain were reported by [49] and focused on the methodology (involving infrared stimulated luminescence (IRSL) signals from K-feldspar) that was used for dating a sequence of aeolian and fluvial deposits as exposed in the sandpit at Mužlja.

In this study, four additional OSL-samples were collected from a sequence of floodplain deposits exposed at a section at Zrenjanin, of which three could be dated using optically stimulated luminescence (OSL) signals from fine-sandy (63-90 µm) quartz. These samples were prepared in the usual manner (HCl, H_2O_2, sieving, density separation, HF) and mounted on the inner 8 mm of 9.7 mm stainless steel discs using silicon oil as adhesive. Luminescence measurements were made using automated Risø readers equipped with blue (470 nm) and IR (870 or 875 nm) LEDs; all luminescence signals were detected through a 7.5 mm thick Hoya U-340 filter. Details on the luminescence equipment can be found in [50] and [51]. The purity

of the quartz grains was confirmed by an OSL IR depletion ratio consistent with 1.0 ± 0.1 [52]. Equivalent dose (D_e) determination was carried out using the single-aliquot regenerative-dose (SAR) protocol as described by [53,54]. Optical stimulation with the blue diodes was for 38 s at 125°C. The initial 0.31 s of the decay curve, minus a background evaluated from the 0.31 - 1.08 s interval, was used in the calculations. The measurement of the test-dose signal was preceded by a cut-heat to 160°C and followed by a high-temperature cleanout by stimulating with the blue diodes for 38 s at 280 °C. D_e's were calculated from the flat 160 - 260°C region in a plot of D_e versus preheat temperature ("preheat plateau"; the duration of the preheat was 10 s). For one of the samples, the dependence of the measured dose on preheat temperature was also investigated through a dose recovery test [54]. Natural aliquots were bleached using the blue LEDs at room temperature (2 times 250 s with a 10 ks pause in between), given a dose close to the estimated D_e, and measured using the SAR protocol as outlined in the above. Three aliquots were measured at each of seven different preheat temperatures in the range of 160 - 280°C. For all samples, a dose recovery test was also performed for a preheat of 220°C only, but using a higher cut-heat to 200°C. Low-level high-resolution gamma-ray spectrometry was used for the determination of the natural dose rate (see [55, 56] for details). For this, the sediment collected around the OSL tubes was dried at 110°C (until constant weight), homogenized and pulverized. A subsample of typically ~140 g was then cast in wax [57] and stored for one month before being measured. The radionuclide activities were converted to dose rates using the conversion factors tabulated by [58]. Based on [59] and [60], a factor of 0.9 (± 5% relative uncertainty) was adopted to correct the external beta dose rates for the effects of attenuation and etching. An internal dose rate of 0.013 ± 0.003 Gy $ka^{-1}$was assumed [61]. Dose rates were corrected for the effect of moisture, assuming a time-averaged moisture content of 20 ± 5 %. The contribution from cosmic rays was calculated following [62]. Uncertainties on the luminescence ages were calculated following the error assessment system proposed by [63] and [64], using contributions from systematic sources of uncertainty as quantified by [56,65].

Preprints (www.preprints.org) | NOT PEER-REVIEWED | Posted: 26 June 2018 doi:10.20944/preprints201806.0430.v1

Peer-reviewed version available at Quaternary 2018, 1, 14; doi:10.3390/quat1020014

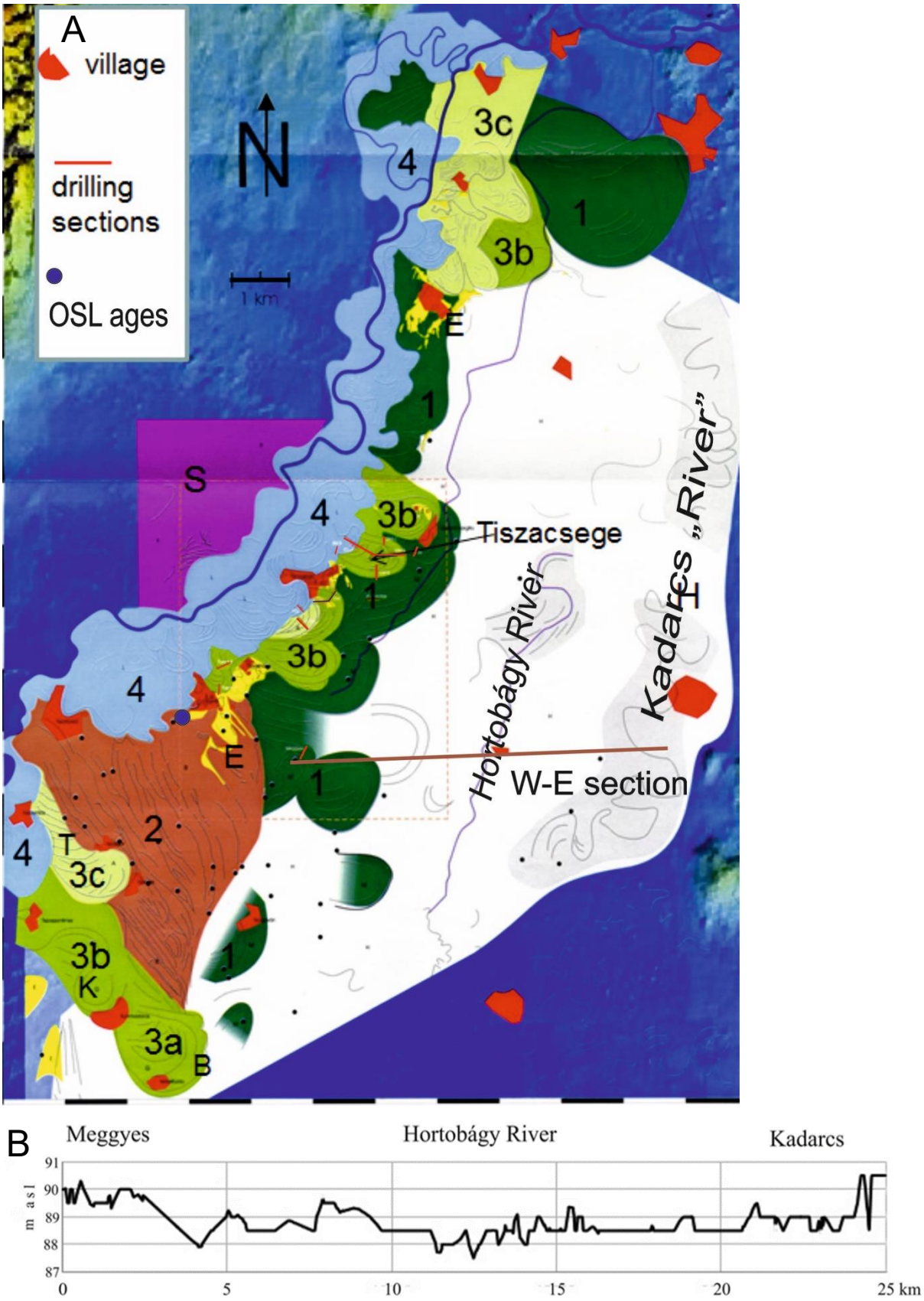

Figure 2 A: Morphological map of the middle Tisza area. H: Hortobagy system; E: aeolian forms; 1-4: fluvial systems (see text); 3a-b-c: Berekfurdo (B)-Kunmadaras (K)-Tiszaörs (T) meanders in lower left corner (from [10]); S: Sajo alluvial fan; W-E section, see B; B:

topographic W-E section through the Hortobagy plain, including the old Kadarcs system and the Meggyes meander (system 1 of the younger valley belt).

4. New results

4.1 Middle Tisza (NE Hungary):

We complete the former description of the middle Tisza system [30] by the sedimentology and morphology of a more upstream large meander near Tiszacsege (Figures 2 and 3). That meander, belonging to system 3b (see below) together with a few neighbouring meanders of similar size (e.g. at Ujszentmargita; Figures 2, and 3), is eroding the sediments of the previous meandering system 1 comprising, for instance, the Meggyes meander (Figures 2 and 3). A detailed drilling section along the axis of the Tiszacsege meander bend shows the development and outlook of a typical meander bend. It consists morphologically of a series of ridges and swales and an outer deep abandoned channel (Figure 3). The latter channel marks the final stage of the meander development before it was cut. The entire area is covered with a veneer of clayey silt, often consisting of alternating laminae of sandy silt and clay, interpreted as flood sediment from the simultaneous and/or younger river. The top of the ridges may be up to 3 m higher than the swales in between. They consist of vertical sets of slightly laminated, fining-up sediment sequences from coarse (gravelly) to fine silty sands (Figure 4), each individual set reaching a maximum thickness (when not eroded) of 2 à 3 m. The depressions in between them show a similar sediment sequence except that the upper clayey-silty cover is generally thicker than on top of the ridges, which means that the topography predating the ultimate flooding of the areas was even more pronounced than it is at present. From the morphology, sedimentology and position within the meander bend, these forms and sediments are obviously interpreted as a series of (high) scroll bars (point bars) leaving a depression successively between each of them. The youngest channel of the system is filled, after abandonment, with maximum 15 m of similar fine-grained sediment as the upper flood sediment that covers the point bars, but more humic and containing molluscs. The pollen diagram of Tiszacsege is located at the maximum curvature of this abandoned channel; it starts in the final phase of the Pleniglacial [30].

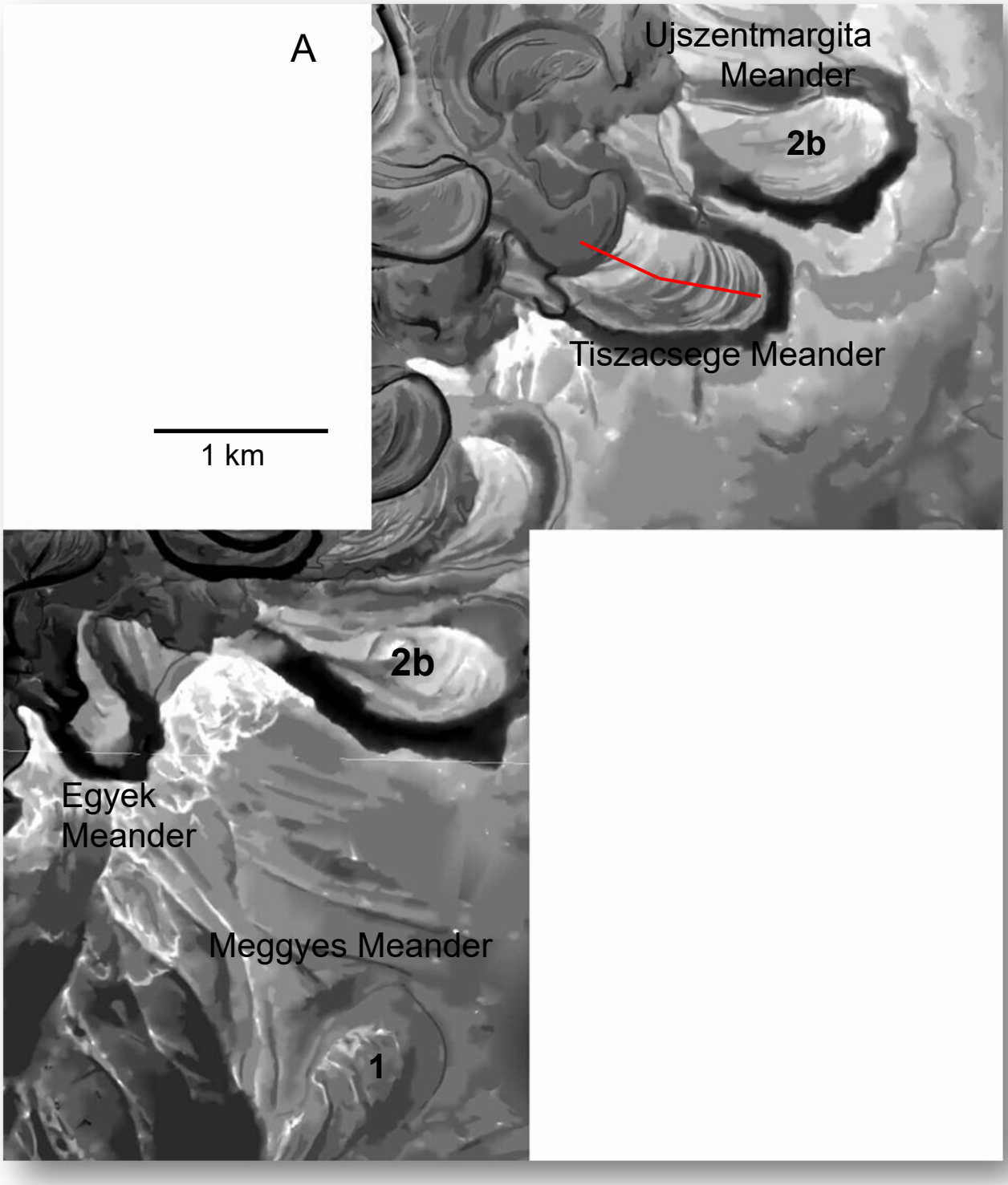

Preprints (www.preprints.org) | NOT PEER-REVIEWED | Posted: 26 June 2018 doi:10.20944/preprints201806.0430.v1

Peer-reviewed version available at Quaternary 2018, 1, 14; doi:10.3390/quat1020014

Figure 3 A: Air photo from study area in the middle Tisza (location see Figure 1). B: Photo shows swale and ridge topography in the meander bend of Tiszacsege.

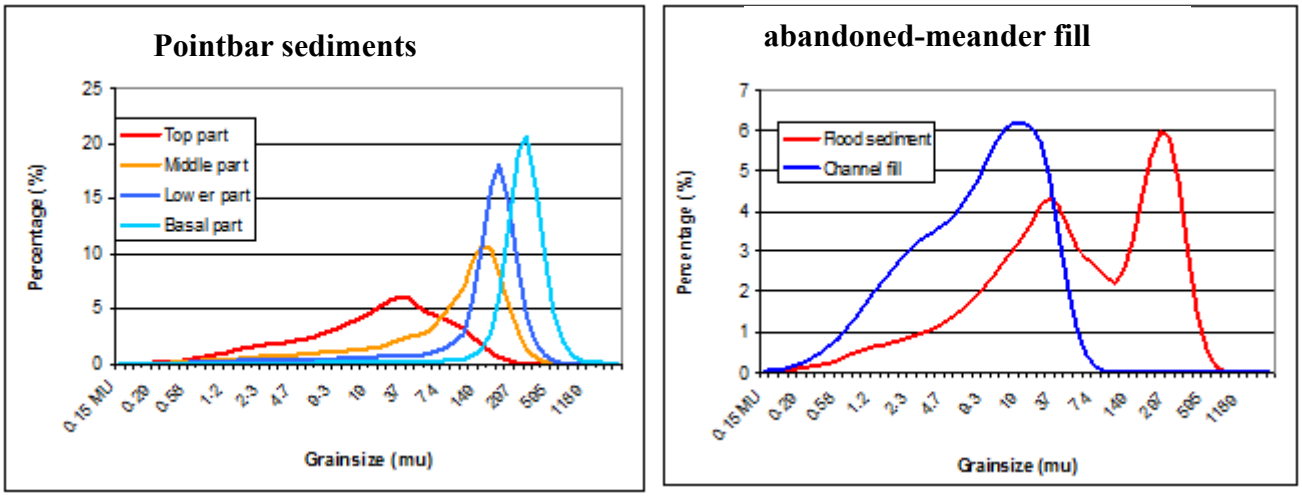

Figure 4 Typical grain-size distributions of point bar, flood and channel fill sediments of the Tiszacsege meander (middle Tisza). The left diagram shows a representative grain-size evolution in one individual point bar (at depths of 6.50, 5.20, 4.60 and 3.80 m). The right diagram shows the grain-size distribution in the centre of the last abandoned channel of max. 15.5 m depth (flood sediment from the upper 2 m, channel fill at c. 8 m depth).

Detailed grain-size information of point bar series and channel fill is represented in Figure 4. Decreasing grainsize typifies the sands of the point bars in upward direction [66]. The upper flood sediments generally contain a fraction with mode around 40 µm (the red (top sediment) curve in the left diagram of Figure 4), which is the typical mode for loess deposits

Preprints (www.preprints.org) | NOT PEER-REVIEWED | Posted: 26 June 2018 doi:10.20944/preprints201806.0430.v1

Peer-reviewed version available at Quaternary 2018, 1, 14; doi:10.3390/quat1020014

in this region [67, 68], thus easily interpreted as reworked (alluvial) loess deposits [69]. In addition, the flood sediment often contains also a sand fraction (most obvious in the right panel of Figure 4) indicating some flow on top of the previous floodplain [69, 70]. The channel fill shows a clear bimodality (Figure 4, right panel): one fraction is a fine silt (c. 19 µm that corresponds with the fine component in the regional loess cover [67, 68] and is preferentially settled in the standing water of the abandoned meander, in contrast to the coarser-grained silt (40 µm) which is dominating in the flood sediments; the second fraction is a clay (c. 2 µm) which can only be deposited by settling in standing water (‘lacustro-aeolian loess’ [69].

4.2 Lower Tisa (Serbia):

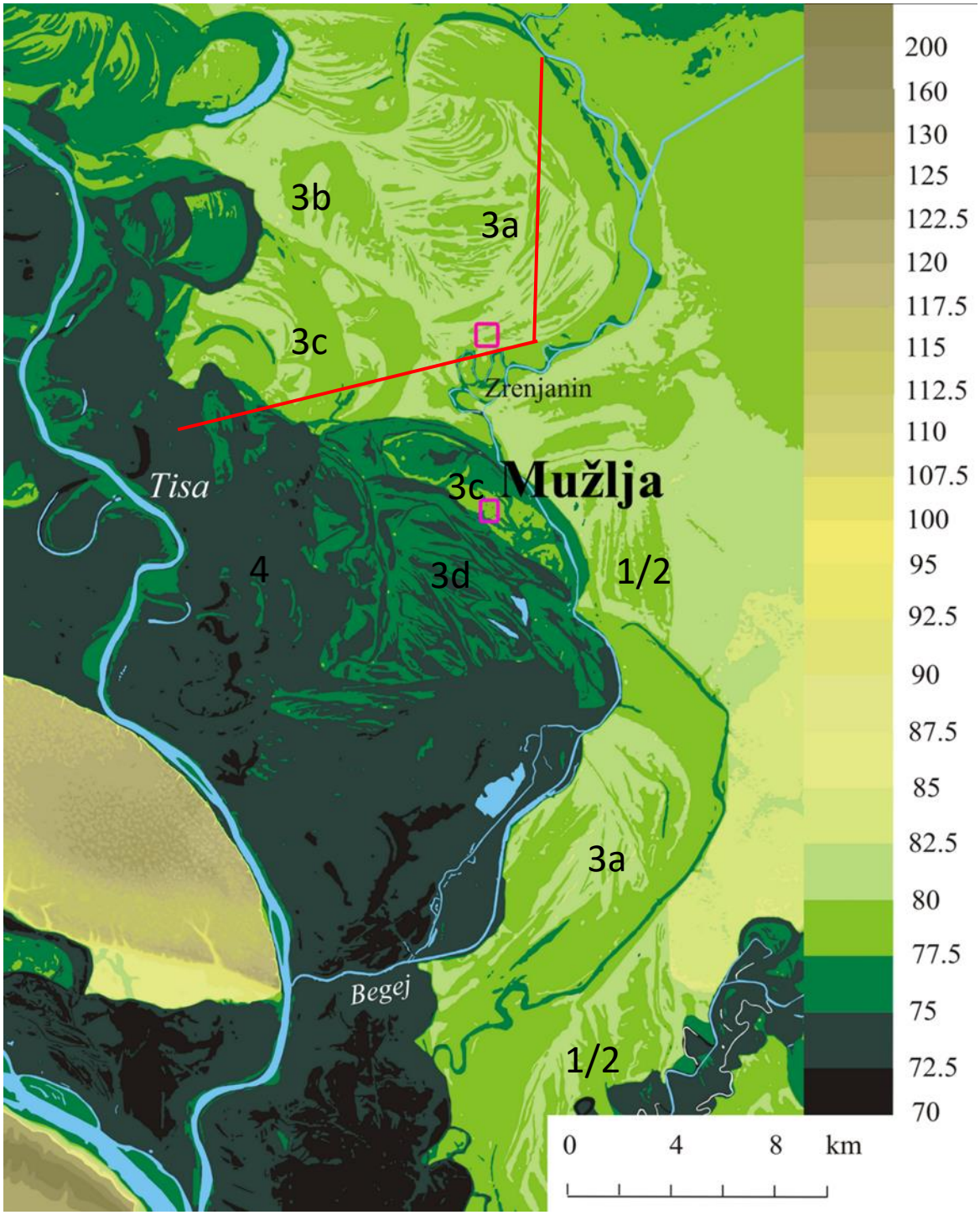

Figure 5 Morphological map of the study area in the lower Tisa comprising the terrace systems 1, 3 and 4 incised in the loess plateaus at both sides of the river. System (2) braided pattern from Hungary (level B, unit 2) is absent here. The squares indicate the locations of the exposures at Zrenjanin and Mužlja.

The former morpho-sedimentary research by [31] is extended here by additional field and laboratory investigations. Three sections approximately perpendicular to the present Tisa River were investigated mainly by hand drillings supplemented with some exposures (unpubl. internal report). Sharply dissecting the Titel plateau in the west (at 110-130 m) and the Tamiš plateau in the east (at >82 m in the east), both consisting of Late Pleistocene loess [68, 71-73], a series of meander systems may be distinguished. The Zrenjanin section is the most representative one, crossing 3 terrace levels (location Figure 5). As in the case of the middle Tisza, the different systems were distinguished by elevation and by erosive meander scarps.

The oldest fluvial series, mainly consisting of large meanders, may be subdivided in systems (1), (3a) and (3b) all situated approximately at the same elevation of c. 79-81 m, a system (3c) slightly lower at 78-79 m, and a youngest one a few m lower (system 3d at c. 75 m). Clearly separated from that series of large meanders is a series of small meanders (system 4), further not subdivided, at 72-75 m elevation (Figure 5).

In general, each terrace level shows the same morpho-sedimentary expression as the Tiszacsege meander described above. Morphologically there is a clear succession of ridges and depressions, interpreted as point bars and inter-bar swales, respectively. Both of them are covered by a sheet of clayey flood sediments. The latter flood sediments are somewhat thicker than in the middle Tisza (1,5 to 3,5 m). The underlying point bar sediments consist of individual sets of 1 to 3 m thick fining-upward sediment ending up at their top in gyttja or clay (in the middle Tisza this very fine top sediments are missing, except in the abandoned channels) and occasionally containing shell debris and coarse sand grains at the bottom. They are interrupted by channels until 12 m deep, often at the outer edge of a terrace level. After abandonment the latter channels are mainly filled with similar fine-grained sediments as the flood cover, i.e. (clayey) silt or fine sand at the base covered by (humic) silt-clay with sand laminae and ultimately clay-silt without sand. The lowest filling sediments may occasionally contain poorly sorted sand beds. For more details, see the discussion of the grain-size data at Zrenjanin below.

Figure 6 Top of the section at Zrenjanin in the upper sediments of a large meander. Notice the chernozem soil at the surface and a soil at 1,7-2,00 m depth with prismatic structure.

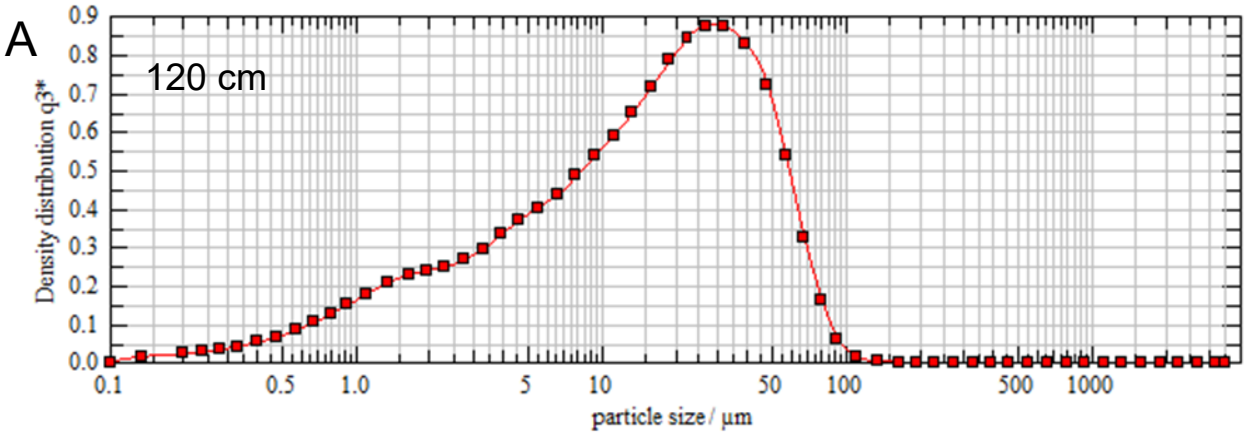

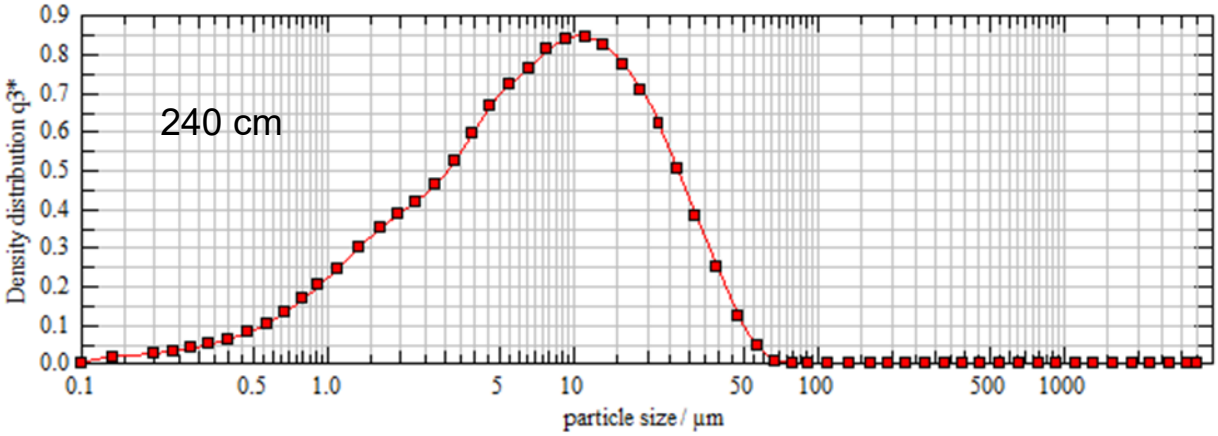

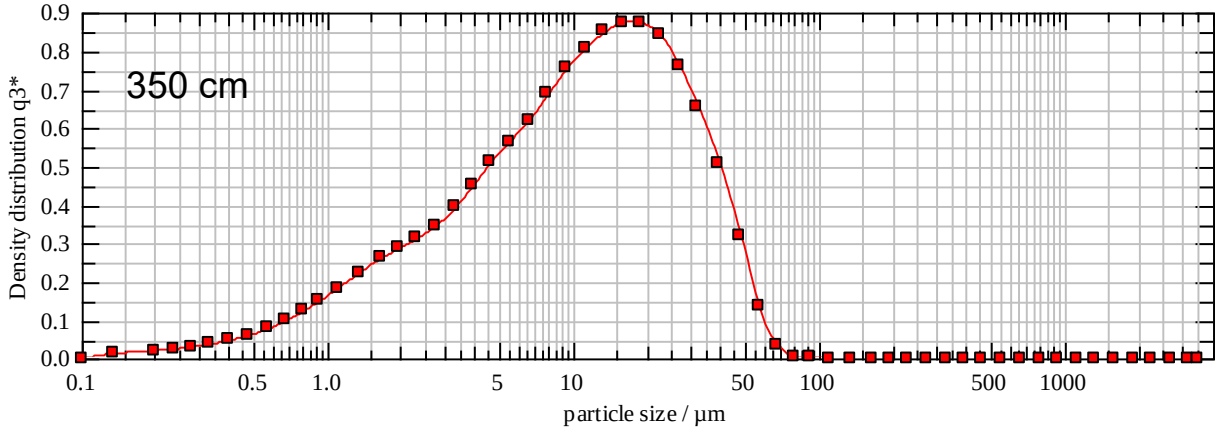

B

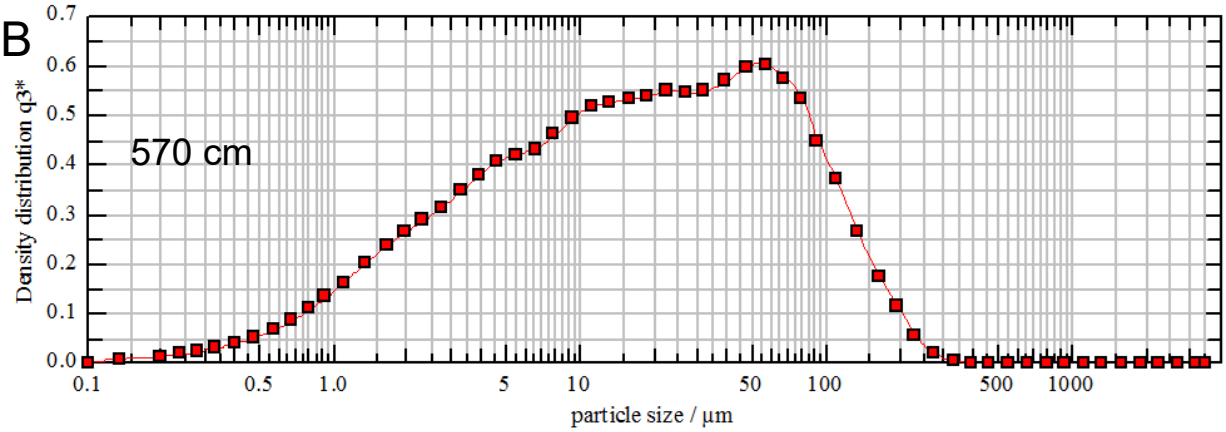

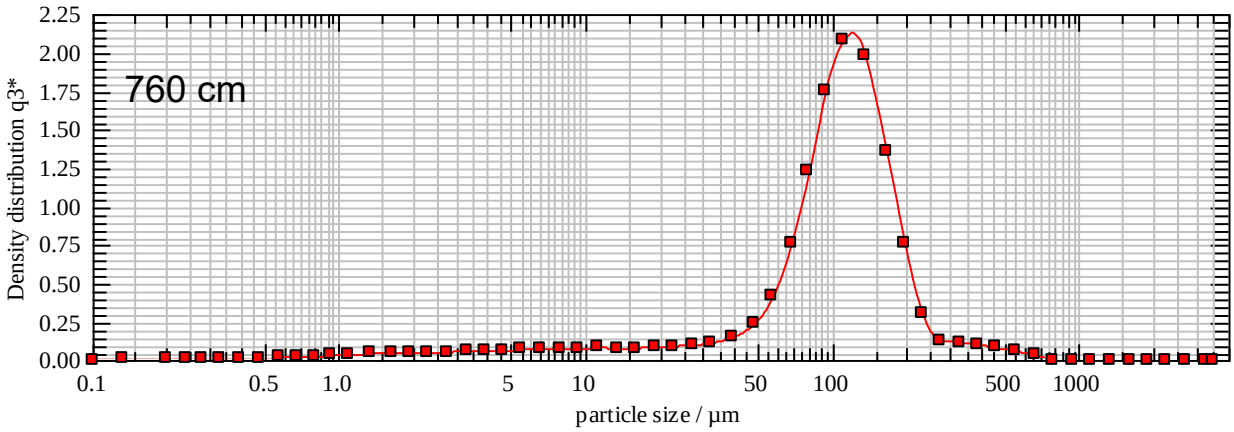

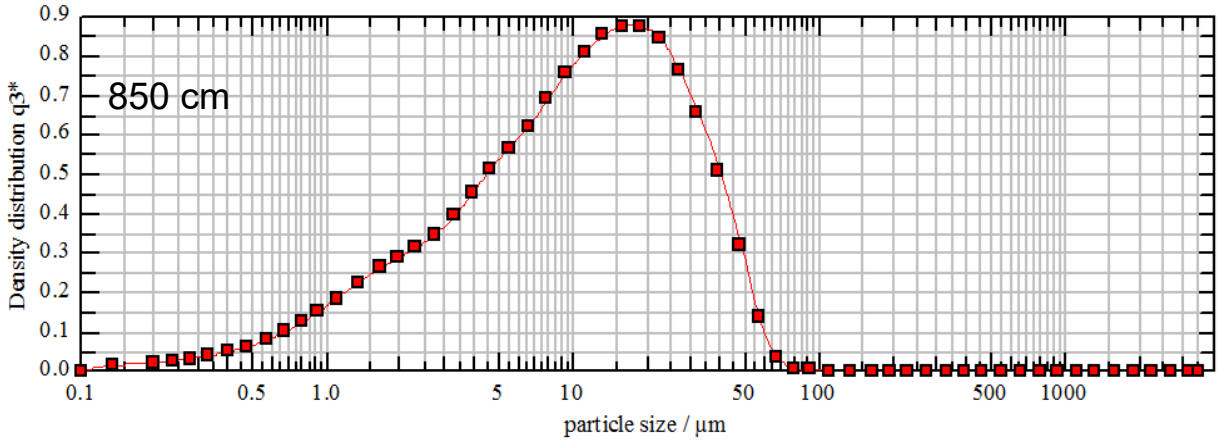

C

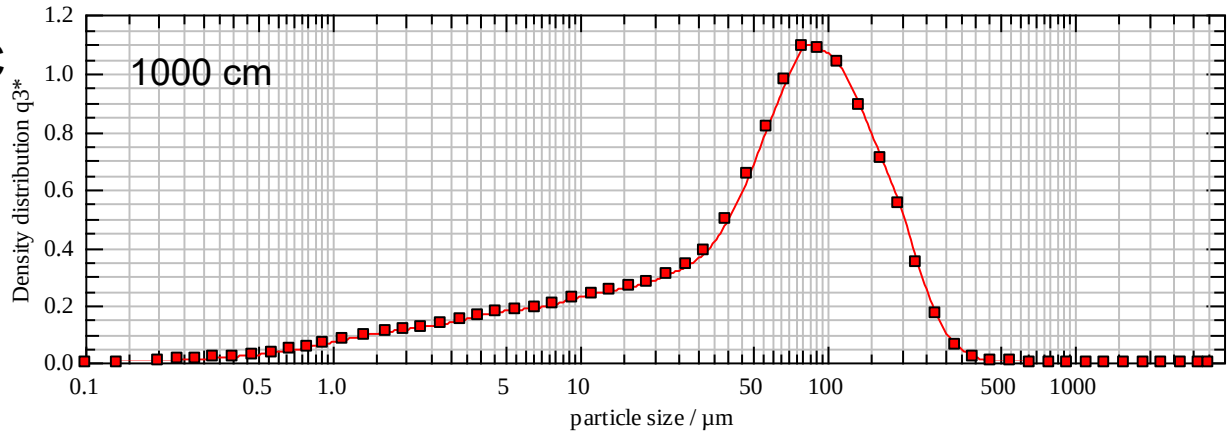

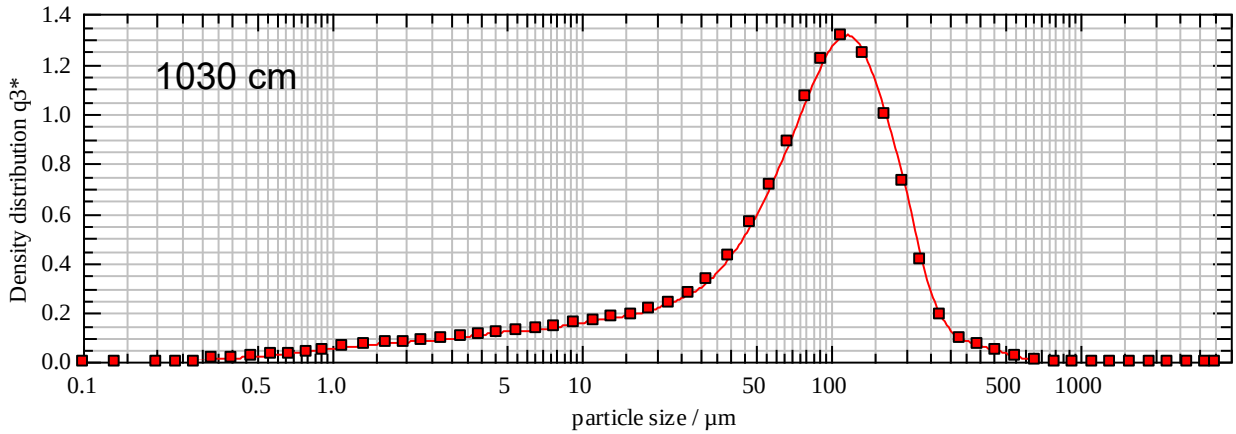

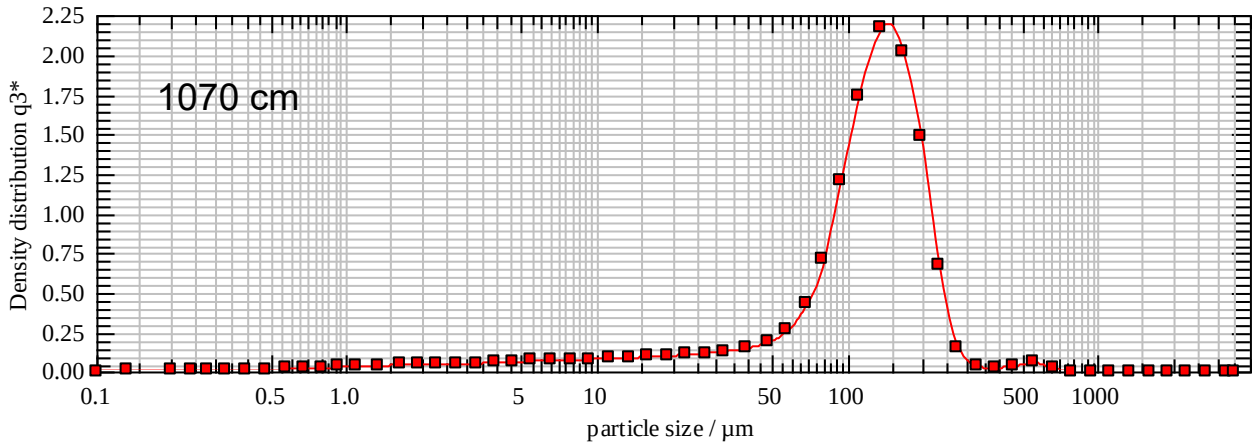

Figure 7 Grain-size distribution curves of the sediments in the meander system of Zrenjanin (location in Figure 5); depths in cm below surface. A: different facies in the exposed upper silty floodplain sediment; B: grain-size distributions from drilled laminated sandy-silty sediment (channel fill) at the same location; C: grain-size distributions from a drilled fining-upward point bar series.

An exposure at Zrenjanin (location Figure 5) enabled the detailed study and sampling of the sedimentary structures in the 2-6.5 m thick, fine-grained sediments that occur at the top of the sediment series in meander system 3a (Figure 6). There is a gradual transition to the underlying sediments, which are more sandy and were cored by hand drilling until a depth of 10.70 m below surface. The sediment series is described according to sedimentary structures and grain-size composition:

0-2.30 m: clay-rich silt (c. 30 % clay) with uniform grain-size composition, modal size of c. 30 µm and almost completely free of sand (Figure 7A). A chernozem soil (1 m thick) is formed at the top while a brown-rusty soil with prismatic structure is present between 1.70 and 2.00 m (Figure 6).

2.30-2.80 m: A clay-silt sediment without any sand and a modal size of 10 µm, horizontally, finely laminated (Figure 7A, 8A). The transition to the overlying sediment is gradual with bimodal laminae, and similarly the transition to the underlying layer is gradual.

2.80- 5.20 m: alternating thin beds consisting of clay-rich fine to medium or coarse silt without sand (350 cm in Figure 7A) and obliquely bedded silty sand layers (up to 20% sand, modal values of 20 and 50 µm) (Figure 8A). The sand beds become thicker towards the base of this unit (ranging from a few cm to a few tens of cm thick) showing small but clear cross-laminated ripples pointing to a westward water flow (fig. 8B). The lower boundary of these sand beds is mostly sharp (erosive). Calcium carbonate nodules are frequently present, as well as micas on the bedding surfaces. A layer between 5.20 and 5.80 m shows a transitional grain size to the underlying layer.

5.80-6.50 m: horizontally, finely laminated, silty fine sands with modal values between 55 and 80 µm (Figure 7B) alternating with silt-clay beds (a few tens of cm thick) with sharp upper boundary. Convoluted deformations at the scale of tens of cm resulting from liquefaction are present in the silt-clay beds; a periglacial origin is not obvious. Gradually changing (6.50-7.00 m) to 7.00-8.70 m: sandy beds coarsening to >100 µm modal value with occasional coarse-sand fraction and decreasing silt and clay content, alternating with silt-clay beds (Figure 7B).

8.70-10.70 m: two clearly developed fining-up sand series (Figure 7C).

The lowest unit (8.70-10.70 m) is interpreted as a typical facies of channel and point bar deposits within an actively meandering system. The facies of heterogeneous, poorly sorted sands and silts between 7.00 and 8.70 m shows characteristics of upper point bar deposits. The upper 6.50 m fine-grained sediments are interpreted as channel fills or accumulation in the floodplain of a meandering system that formed in between the point bars of system 3a (see below and Figure5).

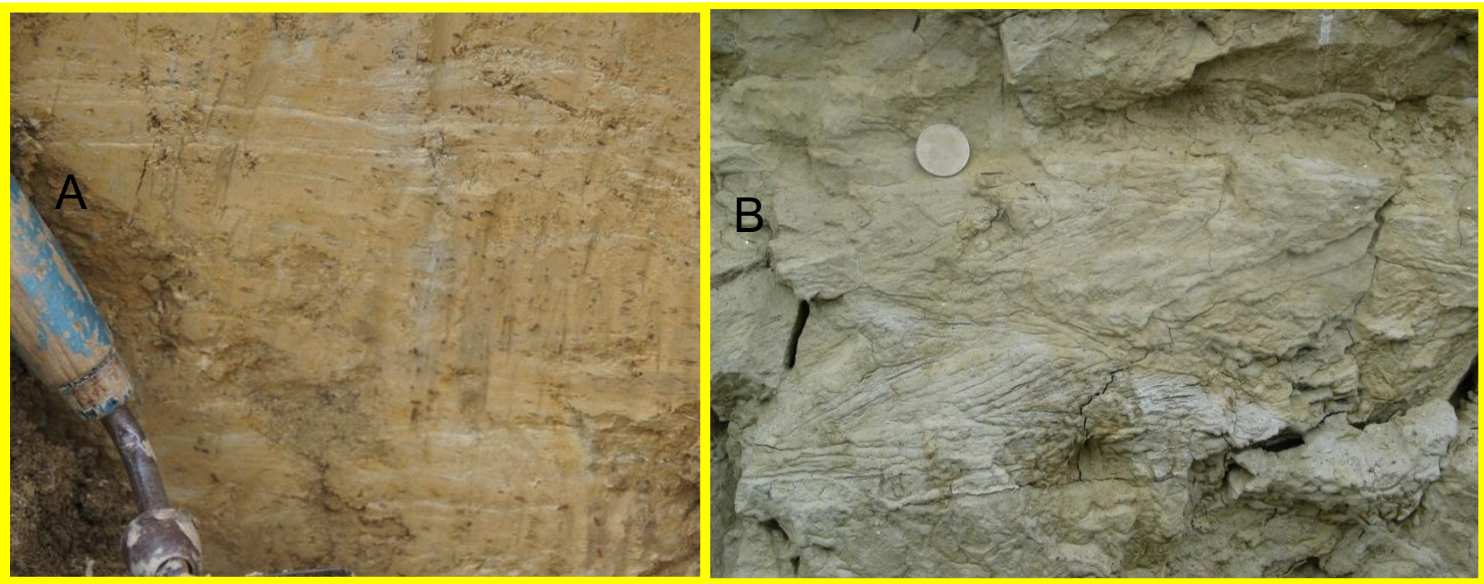

Figure 8 Sedimentary structures in the section at Zrenjanin: A: finely laminated clay-silt (2,30-2,80 m), B: cross-laminated ripple bedding,

Samples for quartz-based SAR-OSL dating were taken at 5.40 m in homogeneous silt-clay, 6.10 m and 6.60 m in cross-laminated sand, and at 6.90 m in a silt-clay bed. The uppermost sample yielded insufficient fine-sandy quartz to allow OSL-analyses. The results for the other three samples are summarised in Table 1. An internally consistent set of OSL-ages was obtained (32-33 ka), showing no variation with depth. Given the depositional context of the samples, and the multiple-grain mode of analysis (see higher) the results are to be interpreted as maximum ages. It has been argued, however, that incomplete resetting is rarely a significant source of inaccuracy for the ages under consideration [74]. A dose-response and OSL-decay (inset) curve for an aliquot of sample GLL-150803 are shown (Figure S1), To describe the dose-response curves, we used either a single, or the sum of two single saturating exponential functions. D_e values exhibit no systematic dependence on preheat temperatures in the range of 160-260°C (see Figure S2); across this region, recycling ratios are generally consistent with 1.0 ± 0.1, and values for recuperation remain comfortably below 0.5% of the sensitivity-corrected natural signal. The dose-recovery test yielded an average measured to given dose ratio (± 1 standard error) of 1.13 ± 0.03 across the 160-260°C preheat temperature range (n = 18; sample GLL-150803; Figure S3). It implies that a known laboratory dose, administered following bleaching but prior to heating, cannot be measured to within – and is systematically overestimated by – about 10%. Increasing the cut-heat temperature to 20°C below the preheat temperature did not improve our ability to recover a dose; a dose recovery test using a preheat temperature of 220°C (chosen as the approximate middle of the preheat plateau) and a cut heat to 200°C yielded a value of 1.15 ± 0.05 (n = 9; three aliquots for each sample). This behaviour, and its relevance as to the accuracy of measurements of natural doses, remains to be understood. Combining these finds with our earlier results [49], indicates

that the possibilities of OSL dating using quartz may be limited; future studies may therefore want to further the investigations into the potential of K-feldspar.

Table 1: Radionuclide concentrations used for dose rate evaluation, estimates of past water content, calculated dose rates, D_e's, and calculated ages (Zrenjanin). The dose rate includes the contributions from internal radioactivity and cosmic rays. The uncertainties mentioned with the D_e and dosimetry data are random; the uncertainties on the ages are the overall uncertainties, which include the systematic errors. All uncertainties represent 1s.

Field Code	*GLL code*	*^{234}Th (Bq kg^{-1})*	*^{226}Ra (Bq kg^{-1})*	*^{210}Pb (Bq kg^{-1})*	*^{232}Th (Bq kg^{-1})*	*^{40}K (Bq kg^{-1})*	*Water content (%)*	*Dose rate (Gy ka^{-1})*	*D_e (Gy)*	*Age (ka)*
ZR 6.10	GLL-150802	33 ± 3	38.5 ± 0.6	35 ± 2	44.0 ± 0.3	605 ± 4	20 ± 5	2.82 ± 0.02	92 ± 5	32 ± 3
ZR 6.60	GLL-150803	29 ± 1	31.5 ± 0.5	34 ± 2	36.6 ± 0.4	445 ± 3	20 ± 5	2.27 ± 0.02	74 ± 3	33 ± 3
ZR 6.90	GLL-150804	31 ± 2	34.7 ± 0.5	33 ± 2	42 ± 0.4	624 ± 4	20 ± 5	2.80 ± 0.03	90 ± 6	32 ± 4

The lateral erosion scar of the meandering system 3d enabled to study an exposure in the sediments of system 3c at Mužlja (location Figure 5). This 4 m deep exposure is located only a few meters from the section that previously has been sampled for luminescence dating [49]. The sediments underlie a point bar of that system. In general, they are finely and horizontally laminated fine-grained sands, occasionally silty and cross-laminated.

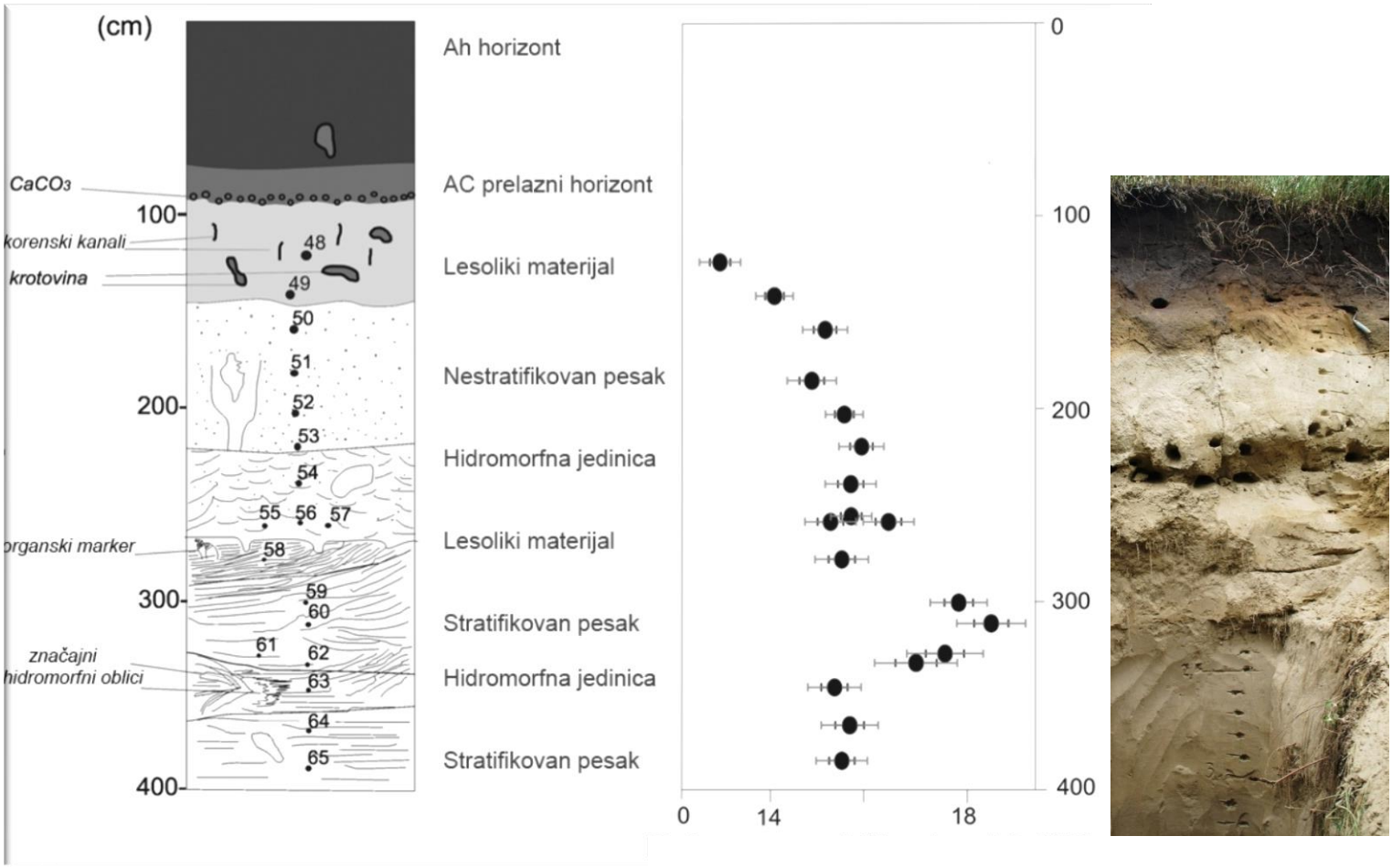

Figure 9 The Mužlja section showing sediments of the meander system 3c (location Fig 5); description of sedimentary structures and lithology, and IRSL dates from [49] with x-axis in ka.

Below a 1 m thick Holocene chernozem soil, in general finely and horizontally laminated fine-grained sand occurs with slightly more silty beds at 1.30-1.50 m and 1.70-1.80 m depth. Slightly coarser sand, mica-rich with low-angle cross-lamination and containing some pebbles of mm size, occurs at 2.70-2.80 m and 3.10-3.25 m depth (Figure 10). The presence of a 2 cm thick, finely laminated, clayey silt bed is striking. The origin of this 4 m sediment series is not really obvious: their spatial and stratigraphic position would suggest a fluvial point bar origin, but no current flow structures were found and a local dune blown up from point bar deposits is not excluded. However, the nearby section used for the OSL-sampling (Figure 9) shows clearer channelling structures (concave-down discontinuous boundaries, cross-lamination of dm size) and ripple cross-lamination, thus favouring a (low-energetic) fluvial nature of the deposits in the exposure.
IRSL-dating of K-feldspar provided an age of 15.3-15.6 ka for the deposition of the point bars of that specific meander system [49; see Figure 9].

5. Identification and age of the different phases of fluvial evolution:

As a result of the dominant regional subsidence of the Pannonian Basin, the different phases of fluvial evolution are only weakly manifested by height differences and no real staircase terrace landscape was formed. Some of these phases terminated their accumulation at similar elevation and can only be distinguished from each other by erosional contacts or dissection of the older fluvial morphological patterns. An additional difficulty in the sedimentary record is that, in general, all sediments of a specific evolution phase are covered by floodplain deposits of (a) younger phase(s) of fluvial activity as a consequence of the subdued morphology. Finally, as discussed extensively by [30], both meander-fill and floodplain deposits may give too old radiocarbon ages due to reworking of older organic deposits.

Originally, the Tisza occupied a position near to the eastern margin of the Pannonian basin during the Early-Middle Pleistocene [35]. Due to relatively more intense subsidence in the central part of the basin, the river shifted this position during the late Pleistocene in a westward direction to its current valley [33]. Remnants of the last drainage system before the Tisza reached its present-day valley occur in a subparallel belt east of the present valley (Kadarcs River), occupied in the Holocene by the Hortobagy River, and consist of a series of sinuous channels (grey shaded areas H in Figure 2).

In the Hungarian sector, the surface of the oldest part of the present-day valley (system 1; meander at Meggyes, Figure 3) is - similar to the precursor of the modern Tisza - morphologically weakly expressed due to a cover of younger vertical floodplain accretion (unit 1 and level A in [30]). Remnants of sinuous channel scars and point-bars with differing orientations suggest formation by a meandering river as the Kadarcs system. The humic clay with soil characteristics at the top of this floodplain deposit yielded uncalibrated radiocarbon ages of 22.2 to 24.7 ka BP for autochthonous organic matter (supported by dating of the alkali extract [30]). Since that alluvial clay-soil complex (unfortunately without pollen) probably represents the ultimate phase of floodplain deposition we infer that the age of activity of this system was prior to that date, i.e. older than c. 28 ka cal BP. The oldest parts of the lower Tisa valley system in the Serbian sector are only represented by two very small areas at c. 80 m altitude (Figure 5: level 1/2). Morphologically, this oldest level of the present-day system

shows alternating parallel ridges and swales with indistinct or slightly curved pattern (Figure 5). No age information is available, preventing correlation with the middle Tisza.

The next and younger phase (2) in the middle Tisza region is represented by a braid plain consisting of straight to slightly curved ridges. The radiocarbon dates from these deposits range from 18,010 BP (bulk detritus) to 13,560 BP (snails) [30], which means a (calibrated) age of c. 17-22 ka (see also discussion below). This system is cutting the large meander system 1. More recently, aeolian sands occurring on top of these fluvial deposits were dated by [36, Figure 8; slightly modified by Novothny, unpubl.) at 21.5-27 ka (OSL/IRSL). System 2 has been interpreted before as the southernmost extension of the Sajo alluvial fan and may thus be of local, rather than general, importance [33, 75].

Then follows a characteristic series of meanders (3) in a belt of the present-day Tisza valley that occurs approximately at the same altitude as the oldest meanders (system 1; level C at 88-90 m in the middle Tisza [30] and at c. 80 m in Serbia) and the braided system 2. The morphology is characterized by well-developed point bars with ridge and swale topography and clear sinuous erosive scars pointing to lateral migration often leading to neck-cut-offs. The point bars consist of fine sandy deposits occurring in a series of fining-upward sequences. Abandoned channels are always filled with, occasionally humic, fine sandy to clayey silts as in Figure 7A. Different generations (3a-d) may be distinguished morphologically in this belt by successive lateral erosion of previous meander remnants and by progressively decreasing meander wave length. Lateral erosion is accompanied with distinct channel incision and the deepest meander channels reach considerable depth (until 15 m). Correlation of remnants of meander generations is not easy, not at least because of the difficulties associated with radiocarbon dating.

Based on the relative magnitude of the meanders and their morphologically relative age, we correlate the oldest and largest meanders of that phase (3a) in the lower and middle Tis(z)a with each other, i.e. the meander of Zrenjanin with the meander of Berekfurdo. The meanders that formed during that first phase have a remarkably great wavelength although exact determination is difficult (in the Hungarian sector estimated at c. 6-10 km at Berekfurdo, and in the Serbian sector at c. 10 km at Zrenjanin); the palaeochannel is up to 600 m wide and locally more than 14 m deep at Berekfurdo in Hungary (Kasse et al 2010) and up to 2 km wide in Serbia. There seems to be a lateral morphological transition with the braided system (2) at Berekfurdo, which could mean that systems 2 and the terminal part of 3a were contemporaneous. The floodplain deposits at a depth of 6 to 7 m at Zrenjanin have been dated by OSL at 32-33 ka. The uncalibrated radiocarbon age of c. 29 ka BP for the meander fill in the Berekfurdo channel [30] fits with the OSL dates obtained at Zrenjanin, but conflicts with younger ages (22-25 ka) of adjacent dissected floodplain deposits (belonging to system 1 according to [30]) and unpublished IRSL dates for the uppermost point bar deposits at Berekfurdo (14.3 ± 1.1 ka to 9.4 ± 2.1 ka; Frechen, pers. comm., January 2003). However, the latter point bar deposits reflect only very weak flow as evidenced by the dominance of clayey flood deposits overlying very thin beds of fine sand without any pebbles (except locally derived clay pebbles), the absence of channelling structures, but frequent occurrence of small ripples draped by clay; thus, they may have been rejuvenated by younger (Lateglacial) fluvial action, which would explain their young age obviously deviating from the older radiocarbon ages. In addition, the older ages of the Berekfurdo meander system (3a) are also inconsistent with the younger radiocarbon age (17-22 ka cal BP; see above) of the older or contemporaneous braided system (2) [30], although older OSL-ages (20 à 27 ka) from that braided system 2 were obtained by [36] (see above.). Anyway, the different datings from Berekfurdo remain inconsistent between each other. Rather than trying to reconcile the different age determinations we favour a more generalized pattern of fluvial evolution of system 3a. It assumes continuous activity at least since c. 32-33 ka until c. 17-22 ka when

river activity slowed down (top of Berekfurdo meander) (Table 2). At that same terminal phase of system 3a the meandering system was supposed to interfinger with braided system 2, which is probably representing the outermost zone of the Sajo alluvial fan (Figure 2). Continuous meandering alluviation over that long period from c. 33 to c. 17 ka may explain the occurrence of many beds dated in that interval, for instance those reported by [36], occurring at different positions in the system. They may even include dated material of 22-25 ka attributed to system 1 by [30]. Moreover, transitions between a braided and meandering pattern exist at present at the Ukrainian-Hungarian border and occurred also during the Late Glacial in the Maros river (tributary of the Tisa near to the Hungarian-Serbian border) [76]. The advantage of this hypothesis of fluvial evolution is that we can assemble in one frame all absolute dates (radiocarbon and OSL) from the two regions within their error bars.

A following, younger phase (3b) within that system of meanders is obviously dissecting meanders of phase 3a. It has distinctly smaller wavelengths than the previous generation 3a, in the range of 4-5 km at Kunmadaras. In the lower Tisa the oldest phase eroding the Zrenjanin terrace is represented by a terrace remnant of very limited extent W of Zrenjanin. The radiocarbon age of the Kunmadaras system is 19.26-16.25 ka BP as derived from the meander fill, but 15.26-13.56 ka BP for adjacent sediments (c. 17-19 ka after calibration). According to [30] the ages of the meander fill are probably a few thousand years too old. The Tiszacsege meander and a series of meanders nearby (of comparable size) may correspond with the Kunmadaras meander; the pollen diagram Tiszacsege (discussed by [30]) shows the fill of a meander scar that started at the final part of the Pleniglacial). Fills of large meanders, radiocarbon dated between 20 and 25 ka, were previously reported by [36, 77,78] in the neighbourhood of Polgar at c. 50 km north of our study area. They could be correlated with phase 3a or 3b.

The next, third phase (3c) has smaller meander wavelengths but still occurs at the same topographic level. It is IRSL-dated for the upper point bar series at Mužlja, giving an age of 15.3-15.6 ka ([49]; Figure 9), which is definitely younger than the Kunmadaras terrace. It may correspond with the Tiszaörs meander (wavelength 3-4 km) of the middle Tisza which is radiocarbon dated between 17.9 and 13.8 ka BP using detritus from within point bar deposits [30]. However, the pollen diagram of the meander fill at Tiszaörs shows that infill started only in the final part of the Late Glacial [30] which is at least much younger than the Tiszacsege meander (system 3b). We assume that the meander may have been active from the end of the Pleniglacial until the Late Glacial after which the pollen registration started and thus – accepting the radiocarbon ages - correlate the Tiszaörs meander with the Muzlja terrace.

In the lower Tisa, a next terrace system W of Mužlja (3d) occurs some 2 m lower (at c. 75 m elevation) than the previous one at Mužlja (3c). The meander size seems again to be somewhat more reduced in comparison with the previous phase. It is not recognized in the study region of the middle Tisza. Taking into account the age of the Mužlja terrace, we infer a Late Glacial age for system 3d (Table 2).

A strikingly abrupt change towards the most recent phase, which dates from the Holocene, is found in the middle Tisza. In that area this system of small meanders (4) is separated from the next older terrace by a sharp scarp of about 4 m. In both areas there is a strong reduction in meander length, channel depth and width (that decreased to 500–400 m) and lateral and vertical erosion of the system. It persisted until pre-modern time, i.e. until human intervention.

Table 2 summarizes the different systems in the present valley belt with their derived ages. Most striking features are the clear phase of incision slightly prior to 33 ka, followed by a rather long period of alluviation in a system of very large meanders (system 3a). This system persisted until c. 17 ka, followed by relatively rapid (relative) decrease of meander size in

Peer-reviewed version available at Quaternary 2018, 1, 14; doi:10.3390/quat1020014

several stages 3b-d ending in the Late Glacial. A sharp decrease of meander size occurred at the transition to the Holocene.

Table 2. Summary of the fluvial systems 1 to 3d, and their periods of activity in the Tis(z)a River.

Fluvial phase	Fluvial systems with type-sites	Periods of activity
3d	Meanders W of Mužlja (lower Tisa)	Late Glacial
3c	Meanders of Tiszaörs (middle Tisza)- Mužlja (lower Tisa)	15,6 ka to start of Younger Dryas
3b	Meanders of Kunmadaras (middle Tisza)	19-17 ka
3a	Meanders of Zrenjanin (lower Tisa)-Berekfurdo (middle Tisza)	From c. 33 to 17 ka
2	'Sajo alluvial fan'- braided	c. (27-)22-17 ka
1	Large meanders of Meggyes	>28 ka

6. Discussion

6.1 General characteristics of the middle and lower Tis(z)a river systems:

The general fluvial pattern is that of a dominantly meandering system in which accumulation and erosion seem to have alternated. The subsidence of the Pannonian Basin led to low river gradients and thus to generally low energy conditions that favoured a meandering river pattern. The accumulative activity is once interrupted by the deep erosion of the meanders just before system 3a (Berekfurdo, Tiszaszege). Its precise age could not be established precisely but is estimated shortly before 33 ka. Similar but possibly slightly earlier than in more northern regions [10], the onset of frozen-ground conditions and delayed response of deteriorating vegetation cover in the Pannonian basin may have induced the considerable erosion before the system 3 alluviation, leading to increased runoff with still low sediment supply [8]. At the time of degradation of frozen soils (towards the end of the Weichselian and/or the transition to the Holocene) and subsequent increase of soil permeability, the runoff decreased, and meanders reduced their dimensions due to lower and more steady discharges [79].

The oldest recorded systems in the present-day valley belt (systems 1 and 3a) date from the end of the Weichselian Middle Pleniglacial and show meandering patterns that are relatively large compared to later meandering patterns [30,33]. Because of a relatively thick cover of fine-grained flood-sediment it is not possible to determine precisely form parameters as wavelength or curvature radius. A rough estimate of that system is between 6 and 10 km wavelength. Postdating the meanders at Berekfurdo and Zrenjanin (3a), the size of the meanders is decreasing successively in the meander systems from 3b to 3 c in the middle Tisza (Kunmadaras and Tiszaörs meanders). In the lower Tisa this evolution from 3b to 3d is less distinct as the preserved terrace remnants are too small to be measured (meanders W of Mužlja). In contrast, the Holocene meanders in both regions are considerably smaller than all pre-Holocene systems. This fact is very common in many river systems [80, 81, 10 and references therein].

Comparable large meanders have been described from the Russian Plain and mid-Russian Uplands by [82-84], as exemplified by the Late Valdaian (~Weichselian) Seim river with meander wavelengths of 5 to 6 km, amplitude of 4 km and channel widths of 15 times the recent ones [82]. In that river the elevation difference between highest levees and deepest point of the palaeo-channel amounts to 14 m. In that same river valley in the southern Russian

Plain, younger meanders with Lateglacial valley fill show a reduction of the wavelength to 1.3 km, while the Holocene meander dimensions decreased considerably [83]. That Holocene size reduction is absent in the northeastern Russian Plain, which is still in the modern permafrost zone [82].

Explaining the large meander sizes requires consideration of the specific energy conditions in the fluvial systems during the Middle Pleniglacial (~MIS 3) and early Late Pleniglacial (~MIS 2). The available energy for meander development is especially determined by the discharge and the river gradient [26, 85]) as applied for the Tisza by [86]. Due to the geographical position of the Tis(z)a within the Pannonian Basin, river slopes are very low (see below). With respect to the runoff in this region, it may further be assumed that in a continental environment the soils were frozen, thus impervious, at least for a considerable part of the year, but especially after the relatively cold winters [2, 28]. These conditions may have been present in the Middle Pleniglacial and even more pronounced during the Late Pleniglacial when this region was situated at the margins of sporadic to discontinuous permafrost [40,41]. In addition, peak discharges may have increased due to the thaw of glacier ice in the Carpathians, feeding the Tisza catchment. Also, the rapid and spatially extensive thaw of snow cover in the low-relief setting of the Hungarian Plain may have contributed to high discharges in spring, as they have been – e.g. – up to 8 times larger at that time than at present in the Russian Plain [82,83]. In the Russian systems, frozen-soil conditions were probably even harsher than in western regions, while the topography was subdued in an environment of thermokarst depressions [84].

Furthermore, it is striking that in the Serbian Tisa and the Russian systems no braided-river patterns are present during the Late Pleniglacial. Also in the middle Tisza, a braided system was only occasionally present (see below). This contrasts with most river systems in other West European cold-temperate regions [10, 22, 87]; more examples in [30, p 192]. Although the impact of frozen soil may have been similar in both regions during that period, the river gradients in West Europe were generally higher, even in lowlands (e.g. 0.2-0.3 $m.km^{-1}$ and c. 0.15 $m.km^{-1}$ for the lower Maas river and the middle Warta river in Poland, respectively [80], versus 0.02 à 0.15 $m.km^{-1}$ for the Tisza river). In addition, braided development requires in general a relatively high sedimentation bedload which is favoured by the absence of vegetation. As the tundra vegetation in West Europe was more sparsely developed, in contrast with the well-developed steppe or even forest-steppic vegetation in central and eastern Europe, it is logic to assume less bedload sediment supply to the rivers in the latter regions. A relatively denser vegetation cover, together with the very low river gradients, may thus explain the absent tendency to a braiding pattern development in those regions during the Late Pleniglacial.

6.2 Intercomparison between the middle and lower Tis(z)a

The general characteristics of stream patterns towards the end of the Last Glacial and the transition to the Holocene are similar in both the middle and lower Tis(z)a in Hungary and Serbia. Despite the difficulties in absolute dating of individual systems and the discontinuous nature of fluvial deposition, the trends in the evolution of the Tis(z)a in Hungary and Serbia occur in a parallel way.

There is one specific difference, however, which is the existence of a braided system (2) during the Late Pleniglacial in the middle Tisza in contrast to the lower Tisa. This braided system in the middle Tisza seems to be of local significance and restricted to a limited period of time. Apart from the theoretical possibility of later removal of braided deposits and river patterns in the lower Tisa, the particular location of that braided system at the southern margin of the alluvial fan at the confluence of the Sajo and Tisza Rivers should be mentioned. In addition, different energy conditions do exist in the two regions. Applying the same theories

of drainage pattern development as described above to explain the dominant meandering systems during the last glacial period, topographical conditions may provide again a plausible explanation for the absence of a braided pattern in the lower Tisa. Especially striking is the strongly reduced longitudinal gradient in Serbia, which at present is 1.86 cm/km [31], when compared to the gradient in the middle Tisza of 15 cm/km in central to north Hungary [30], that gradually diminishes to 5-10 cm/km in a zone of intense subsidence in south-eastern Hungary [35]. In contrast, it is not probable to invoke a substantially different vegetation cover between the latter two regions. Thus, the strongly reduced stream power in a downstream direction is supposed to be the main reason for the persistent formation of a meandering pattern, that is not interrupted by braiding, in the lower Tisa during the Late Pleniglacial.

As a general conclusion and a result of the further studies of the Tis(z)a system in Hungary and Serbia, the importance of timescale, as described by [5] is confirmed here. In the long term, the tectonic framework (basin development) and resulting topography have determined the available energy in this fluvial system. At a shorter timescale, climatic conditions (including their effects on vegetation and soil frost) have left a distinct imprint. And finally looking at more detailed spatial and temporal scales, local variations of topography and sediment availability may be responsible for further shaping the river morphology [22, 80] next to intrinsic variables as thresholds and delay times.

7. Conclusions

Several characteristics of fluvial development found in the continental low-relief setting of the Tis(z)a river, are identical to the cold-temperate conditions in the West-European lowlands. In this respect, the sharp decrease in meander size at the Weichselian to Holocene transition is striking. But there are also a few differences, such as the near absence of braided river patterns and the existence of exceptionally large meanders during the Weichselian Middle and Late Pleniglacial.

Previous studies have frequently stressed the importance of climate and tectonic movement as external factors in fluvial morphological development. This study of the Tis(z)a valley illustrates that, for a reliable understanding of fluvial evolution, the impact of climate on fluvial processes and morphology cannot be limited to general estimates or averages but also needs to be effectively specified in detail, for instance including the continental conditions with cold winters and relatively warm summers in the Tis(za) catchment and in the Russian plain. In addition, they have to be supplemented with indirect climate variables (as vegetation, frozen soil and snow cover), while the impact of tectonic subsidence, and its variability within one catchment as the Tis(z)a, has to be specified in semi-direct variables as the longitudinal river gradient and relief intensity. This study confirms the impact of varying conditions of climate and topography at a local and regional level on fluvial development.

Acknowledgements

DV gratefully acknowledges financial support from the Research Foundation Flanders (FWO-Vlaanderen) and the UGent Laboratory of Mineralogy and Petrology, as well as the technical assistance of Ann-Eline Debeer. Field work has been carried out with the help of students from the Vrije Universiteit Amsterdam in the framework of their BSc or Msc thesis. We thank M. Frechen for providing luminescence measurements from the middle Tisza in 2003, and A. Novothny for communicating recent unpublished OSL-dates from the middle Tisza region.

Supplementary materials:

The following are available online at www.mdpi.com/

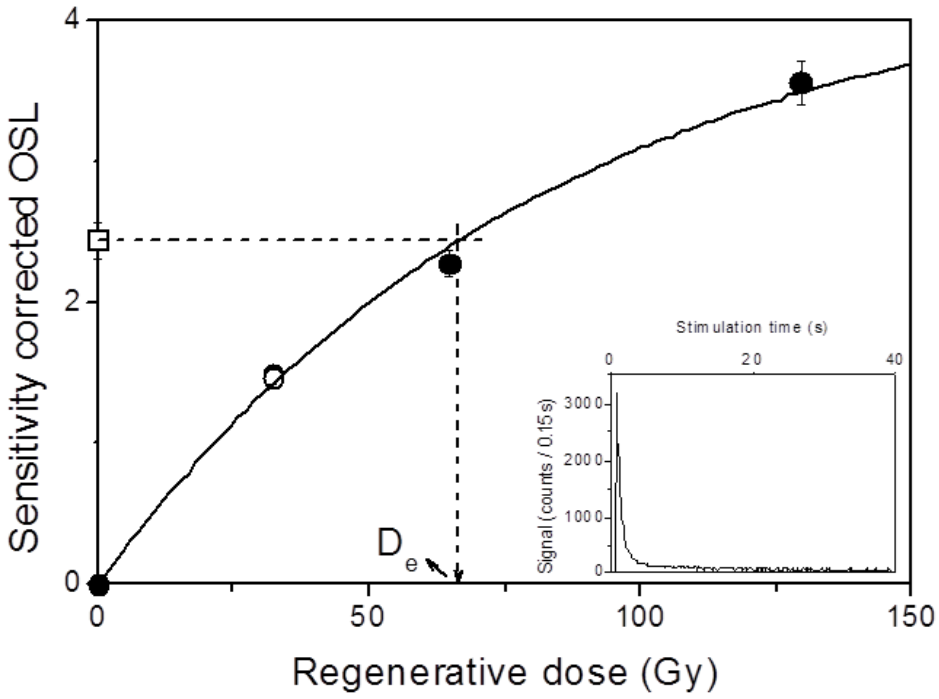

Fig S1. Illustrative dose-response and luminescence decay curve (inset) for an aliquot of quartz grains extracted from sample GLL-150803. The filled circles show the sensitivity-corrected responses to several regenerative doses; the dose-response (solid line) was represented by a single saturating exponential. The open circle represents a repeat measurement of the response to the regenerative dose that was administered first (recycling point). The equivalent dose (D_e) is obtained by interpolating the sensitivity-corrected natural OSL signal (open square) on the dose-response curve.

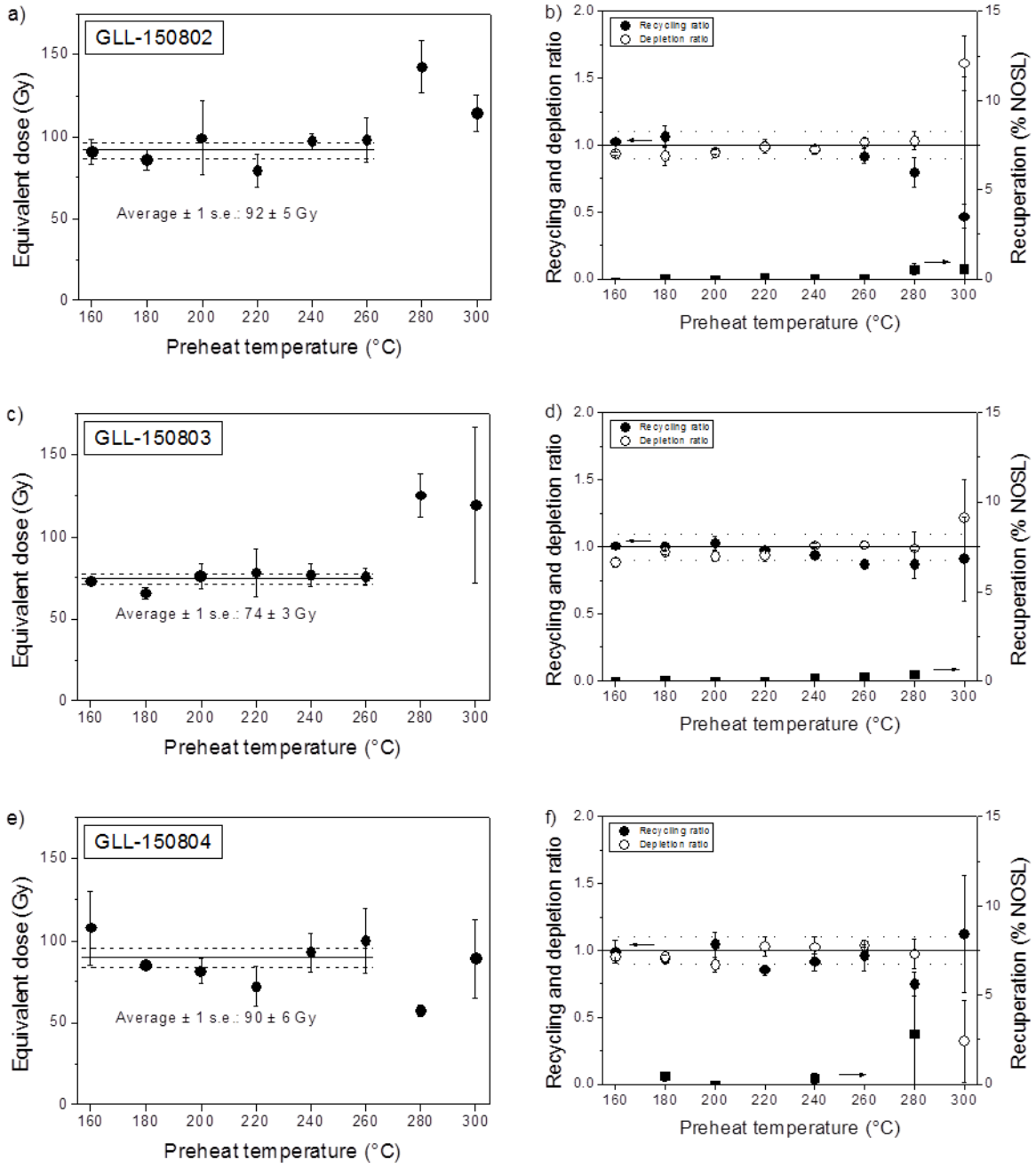

Fig S2. Dependence of equivalent dose on preheat temperature (a, c, e). Each data point represents the average of three measurements; error bars represent 1 standard error (s.e.). The solid and dashed lines represent the unweighted average ± 1 standard error over the 160-260°C temperature region. Figs b, d and f show the corresponding recycling (solid circles) and OSL IR depletion (open circles) ratios (left hand axis) and values for recuperation (solid squares; right hand axis) expressed as a % of the corrected natural OSL signal. The solid and dotted lines (eye guides) represent ratios equal to 1.0 ± 0.1.

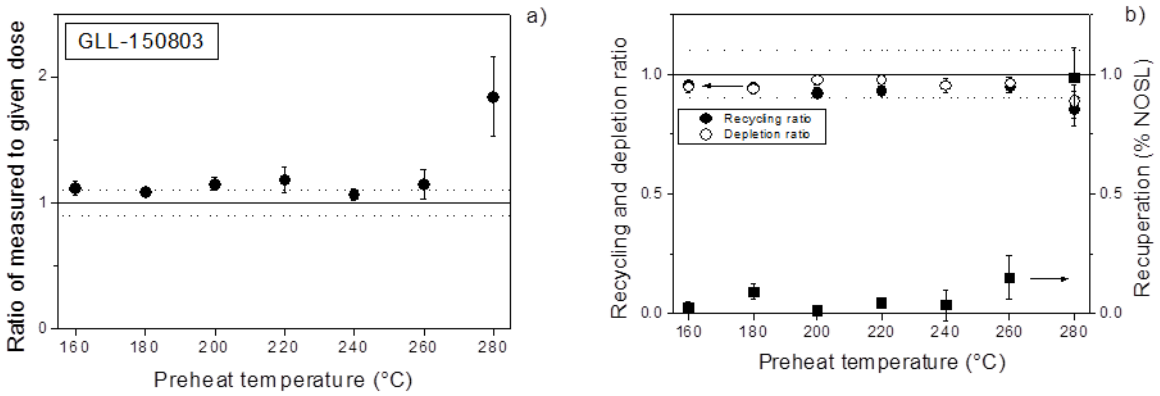

Fig S3. a) Ratios of measured to given dose (dose recovery data) as a function of preheat temperature for sample GLL-150803. Each data point represents the average ± 1 s.e. of three measurements. b) Corresponding recycling and OSL IR depletion ratios (left hand axis) and recuperation values (right hand axis). The solid and dotted lines (eye guides) represent ratios equal to 1.0 ± 0.1.

Author contributions: conceptualization, field data collection, interpretation, writing original draft, J.V., K.K. and G.G.; OSL-dating, D.V. and D.P.
The authors declare no conflict of interest.

References

[1] Büdel, J. Klima-Geomorphologie. Gebrüder Bornträger: Berlin, Germany, 1977; 304 pp.

[2] Vandenberghe, J. The relation between climate and river processes, landforms and deposits during the Quaternary. Quatern. Int. 2002, 91, 17-23.

[3] Starkel L. Climatically controlled terraces in uplifting mountain areas. Quat. Sci. Rev. 2003, 22, 2189-2198.

[4] Vandenberghe, J. Changing fluvial processes under changing periglacial conditions. Zeitschr. f. Geomorphol., Suppl. Bd. 1993, 88, 17-28.

[5] Vandenberghe, J. Timescales, climate and river development. Quat. Sci. Rev. 1995, 14, 631-638.

[6] Bridgland, D.R.; Allen, P. A revised model for terrace formation and its significance for the early middle Pleistocene terrace aggradations of north-east Essex, England. In *The early Middle Pleistocene in Europe;* Turner, C., Ed.; Balkema; Rotterdam, The Netherlands, 1996, pp. 121-134.

[7] Maddy, D.; Bridgland, D.; Westaway, R. Uplift-driven valley incision and climate-controlled river terrace development in the Thames Valley, UK. Quat. Int. 2001, 79, 23–36.

[8] Vandenberghe, J. The fluvial cycle at cold-warm-cold transitions in lowland regions: a refinement of theory. Geomorphology 2008, 98, 275-284.

[9] Vandenberghe, J. River terraces as a response to climatic forcing: formation processes, sedimentary characteristics and sites for human occupation. Quat. Int. 2015. 370, 3-11.

[10] Mol, J.; Vandenberghe, J.; Kasse, C. River response to variations of periglacial climate. Geomorphology 2000, 131–148.

[11] Pan, B., Su, H., Hu, Z., Hu, X., Gao, H., Li, J., Kirby, E., 2009. Evaluating the role of climate and tectonics during non-steady incision of the Yellow River: evidence from a 1.24 Ma terrace record near Lanzhou, China. Quaternary Science Reviews 28, 3281-3290.

[12] Wang, X., Van Balen, R., Yi, S., Vandenberghe, J., Lu, H., 2014. Differential tectonic movements in the confluence area of the Huang Shui and Huang He rivers (Yellow River), NE Tibetan Plateau, as inferred from fluvial terrace positions. Boreas 43, 469-484.

[13] Kemp, J., Pietsch, T., Gontz, A. and Oley,J. 2017 Lacustrine-fluvial interactions in australia's Riverine Plains. Quaternary Science Reviews 166, 352-362.

[14] Marsh, P. and Woo, M.K. 1981: Snowmelt, glacier melt and High Arctic streamflow regimes. Canadian Journal of Earth Sciences 18, 380-1384.

[15] Cordier, S., Frechen, M., Harmand, D. 2014 Dating fluvial erosion: fluvial response to climate change in the Moselle catchment (France, Germany) since the Late Saalian. Boreas 43, 450-468.

[16] Cordier, S.; Adamson, K.; Delmas, M.; Calvet, M.; Harmand, D. Of ice and water: Quaternary fluvial response to glacial forcing. Quat. Sci. Rev. 2017, *166*, 57-73; http://dx.doi.org/10.1016/j.quascirev.2017.02.006

[17] Ballantyne, C. K. A general model of paraglacial landscape response. The Holocene 2002, *12*, 371–376.

[18] Owczarek, P.; Nawrot, A.; Migala, K.; Malik, I.; Korabiewski, B. Floodplain responses to contemporary climate change in small High-Arctic basins (Svalbard, Norway). Boreas 2014, DOI:10.1111/bor.12061.

[19] Dogan,U. Fluvial response to climate change during and after the Last Glacial Maximum in Central Anatolia,Turkey. Quat. Int. 2010, *222*, 221–229.

[20] Avcin, N.; Vandenberghe, J.; van Balen, R.T.; Kıyak, N.; Öztürk, T. Tectonic and Climatic Controls on Quaternary Fluvial Processes and Terrace Formation in a Mediterranean Setting: the Göksu River, Southern Anatolia. Quat. Res. (under review).

[21] Hughes, K.; Croke, J. How did rivers in the wet tropics (NE Queensland, Australia) respond to climate changes over the past 30000 years? J. Quat. Sci. 2017, doi 10.1002/jqs.2956.

[22] Kasse, C. Depositional model for cold-climate tundra rivers. In *Palaeohydrology and Environmental Change*; Benito, G., Baker, V.R., Gregory, K.J., Eds.; Wiley and Sons; Chichester, UK, 1998, pp. 83-97.

[23] Rose, J.; Meng, X. River activity in small catchments over the last 140 ka, North-east Mallorca, Spain. In *Fluvial processes and environmental change*; Brown, A.G., Quine, T.A., Eds.; Wiley & Sons; Chichester, UK; 1999, pp. 91-102.

[24] Olszak, J. Evolution of fluvial terraces in response to climate change and tectonic uplift during the Pleistoce: Evidence from Kamienica and Ochotnica River valleys (Polish Outer Carpathians). Geomorphology 2011, *129*, 71-78.

[25] Stange, K.M.; van Balen, R.T.; Carcaillet, J.; Vandenberghe, J. Terrace staircase development in the Southern Pyrenees Foreland: Inferences from 10Be terrace exposure ages at the Segre River. Global Planet. Change 2013, *101*, 97-112.

[26] Schumm, S. The fluvial system; Wiley-Interscience: New York, USA, 1977, 338 pp.

[27] Van Huissteden, J. Tundra rivers of the Last Glacial: sedimentation and geomorphological processes during the Middle Pleniglacial in the Dinkel Valley (eastern Netherlands). Meded. Rijks Geol. Dienst. 1990, *44*, 3-138.

[28] Vandenberghe, J. A typology of Pleistocene cold-based rivers. Quat. Int. 200, *179*, 111-121.

[29] Bridgland, D.R.; Westaway, R. Preservation patterns of Late Cenozoic fluvial deposits and their implications: results from IGCP 449. Quat. Int. 2008, *189*, 5–38.

[30] Kasse, C.; Bohncke, S.J.P.; Vandenberghe, J.; Gabris, G. Fluvial style changes during the last glacial - interglacial transition in the middle Tisza valley (Hungary). Proc. Geologists' Ass. 2010, *121*, 180-194.

[31] Popov, D.; Markovic, S.; Strbac, D. Generations of meanders in Serbian part of Tisa valley. Geographical Institute 'Jovan Cvijic' SASA, Collection of papers 2008, *58*, 29-41.

[32] Nádor, A.; Lantos, M.; Tóth-Makk, Á.; Thamó-Bozsó, E. Milankovitch-scale multi-proxy records from fluvial sediments of the last 2.6 Ma, Pannonian Basin, Hungary. Quat. Sci. Rev. 2003, *22*, 2157-2175.

[33] Gabris, G.; Nador, A. Long-term fluvial archives in Hungary: response of the Danube and Tisza rivers to tectonic movements and climatic changes during the Quaternary: a review and new synthesis. Quat. Sci. Rev. 2007, *26*, 2758-2782.

[34] Timar, G.; Sümegi, P.; Horvath, F. Late Quaternary dynamics of the Tisza river: evidence of climatic and tectonic controls. Tectonophysics 2005, *410*, 97-110.

[35] Nádor, A.; Thamó-Bozsó, E.; Magyari, A.; Babinszki, E. Fluvial responses to tectonics and climate change during the Late Weichselian in the eastern part of the Pannonian Basin (Hungary). Sedim. Geol. 2007, *201*, 174-192.

[36] Gabris, G.; Horvath, E.; Novothny, A.; Ruszkiczay-Rüdiger, Z. Fluvial and Aeolian landscape evolution in Hungary- results of the last 20 years research. Neth. J. Geosci. 2012, *91-1/2*, 111-128.

[37] Willis, K.J.; Rudner, E.; Sümegi, P. The Full-Glacial Forests of Central and Southeastern Europe. Quat. Res. 2000. *53-2*, 203-213.

[38] Sümegi, P.; Krolopp, E. Quatermalacological analyses for modelling of the Upper Weichselian paleoenvironmental changes in the Carpathian Basin. Quat. Int. 2002, *91*, 53-63.

[39] Bacso, N. Climate of Hungary; Akademiai Kiado, Budapest, Hungary, 1959, 302 pp. (in Hungarian).

[40] Fábián S.A.; Kovács, J.; Varga, G.; Sipos, G.; Horváth, Z.; Thamó-Bozsó, E.; Tóth, G. Distribution of relict permafrost features in the Pannonian Basin, Hungary. Boreas 2014, *43(3)*, 722–732.

[41] Vandenberghe, J.; French, H.M.; Gorbunov, A.; Marchenko, S.; Velichko, A.A.; Jin, H.; Cui, Z.; Zhang, T.; Wan, X. The Last Permafrost Maximum (LPM) map of the Northern Hemisphere: permafrost extent and mean annual air temperatures, 25–17 ka BP. Boreas 2014, *43*, 652–666.

[42] Royden, L.H.; Horvath, F. The Pannonian Basin. A case study in basin evolution. AAPG Memoirs 1988, *45*, 394 pp.

[43] Horvath, F.; Cloetingh, S. Stress induced late-stage subsidence anomalies in the Pannonian Basin. In *Dynamics of extensional basins and inversion tectonics*; Cloetingh, S., Ben Avraham, Z., Sassi, W., Horvath, F., Eds.; Tectonophysics 1996, *266*, 287-300.

[44] Bada, G.; Horvath, F. On the structure and tectonic evolution of the Pannonian Basin and surrounding orogens. Acta Geol. Hung. 2001, *44*, 301-327.

[45] Pecsi, M. Entwicklung und Morphologie des Donautales in Ungarn; Akademiai Kiado, Budapest, Hungary, 1959; 359 pp. (in Hungarian).

[46] Thamo-Bozso, E.; Murray, A.A.; Nador, A.; Magyari, A.; Babinszki, E. Investigation of river network evolution using luminescence dating and heavy-mineral analysis of Late Quaternary fluvial sands from the Great Hungarian Plain. Quat. Geochronol. 2007, *2*, 168-173.

[47] Gabris, G. Pleistocene evolution of the Danube in the Carpathian Basin. Terra Nova 1994, *6*, 495-501.

[48] Konert, M.; Vandenberghe, J. Comparison of laser grain size analysis with pipette and sieve analysis: a solution for the underestimation of the clay fraction. Sedimentology 1997, *44*, 523-535.

[49] Popov, D.; Vandenberghe, D.A.G.; Marković, S.B. Luminescence dating of fluvial deposits in Vojvodina, N Serbia: First results. Quat. Geochronol. 2012a., *13*, 42-51.

[50] Bøtter- Jensen, L.; Andersen, C.E.; Duller, G.A.T.; Murray, A.S. Developments in radiation, stimulation and observation facilities in luminescence measurements. Radiation Measurements 2003, *37*, 535-541.

[51] Lapp, T.; Kook, M.; Murray, A.S.; Thomsen, K.J.; Buylaert, J.-P.; Jain, M. A new luminescence detection and stimulation head for the Risø TL/OSL reader. Radiation Measurements 2015, *81*, 178-184.

[52] Duller, G.A.T. Distinguishing quartz and feldspar in single grain luminescence measurements. Radiation Measurements 2003, *37*, 161-165.

[53] Murray, A.S.; Wintle, A.G. Luminescence dating of quartz using an improved single-aliquot regenerative-dose protocol. Radiation Measurements 2000, *32*, 57-73.

[54] Murray, A.S.; Wintle, A.G. The single aliquot regenerative dose protocol: potential for improvements in reliability. Radiation Measurements 2003, *37*, 377-381

[55] Hossain, S.M. A critical comparison and evaluation of methods for the annual radiation dose determination in the luminescence dating of sediments. PhD thesis, Ghent University, 2003.

[56] Vandenberghe, D. Investigation of the optically stimulated luminescence dating method for application to young geological samples. PhD thesis, Ghent University, 2004.

[57] De Corte, F.; Vandenberghe, D.; De Wispelaere, A.; Buylaert, J.-P.; Van den haute, P. Radon loss from encapsulated sediments in Ge gamma-ray spectrometry for the annual radiation dose determination in luminescence dating. Czech J. Physics 2006, *56*, D183-D194.

[58] Adamiec, G.; Aitken, M. Dose-rate conversion factors: update. Ancient TL 1998, *16*, 37-50.

[59] Mejdahl, V. Thermoluminescence dating: beta-dose attenuation in quartz grains. Archaeometry 1979, *21*, 61-72.

[60] Aitken, M.J. Thermoluminescence Dating: Academic Press Inc., London, UK, 1985; 359pp.

[61] Vandenberghe, D.; De Corte, F.; Buylaert, J.-P.; Kucera, J.; Van den haute, P. On the internal radioactivity in quartz. Radiation Measurements 2008, *43*, 771-775.

[62] Prescott, J.R.; Hutton, J.T. Cosmic ray contributions to dose rates for luminescence and ESR dating: large depths and long-term time variations. Radiation Measurements 1994, *23*, 497-500.

[63] Aitken, M.J. Thermoluminescence age evaluation and assessment of error limits: revised system. Archaeometry 1976, *18*, 233-238.

[64] Aitken, M.J.; Alldred, J.C. The assessment of error limits in thermoluminescence dating. Archaeometry 1972, *14*, 257-267.

[65] Vandenberghe, D.; Kasse, C.; Hossain, S.M.; De Corte, F.; Van den haute, P.; Fuchs, M.; Murray, A.S. Exploring the method of optical dating and comparison of optical and 14C ages of Late Weichselian coversands in the southern Netherlands. J. Quat. Sci. 2004, *19*, 73-86.

[66] Vandenberghe, J.; Bohncke, S.; Lammers, W.; Zilverberg, L. Geomorphology and palaeoecology of the Mark valley (southern Netherlands). I Geomorphological valley develop¬ment during the Weichselian and Holocene. Boreas 1987, *16*, 55-67.

[67] Novotny, A.; Frechen, M.; Horvath, E.; Wacha, L.; Rolf, C. Investigating the penultimate and last glacial cycles of the Süttö loess section (Hungary) using luminescence dating, high-resolution grain size, and magnetic susceptibility data. Quat. Int. 2011, *234*, 75-85.

[68] Bokhorst, M.; Vandenberghe, J.; Sümegi, P.; Lanczont, M.; Gerasimenko,N.P.; Matviishina, Z.N.; Markovic, S.B.; Frechen, M. Atmospheric circulation patterns in Central and Eastern Europe during the Weichselian Pleniglacial inferred from loess grain-size records. Quat. Int. 2011, *234*, 62-74.

[69] Vandenberghe, J.; Sun, Y.; Wang, X.; Abels, H.A.; Liu, X. Grain-size characterization of reworked fine-grained aeolian deposits. Earth Science Reviews 2018, *177*, 43-52.

[70] Wang, X.; Ma, J.; Yi, S.; Vandenberghe, J.; Dai, Y.; Lu, H. Interaction of fluvial and aeolian sedimentation processes and response to climate change since the last glacial in a semi-arid environment along the Yellow River. Quaternary Research 2018, http://dx.doi.org/10.1017/qua.2018.22.

[71] Marković, S.B.; Bokhorst, M.; Vandenberghe, J.; McCoy, W.D.; Oches, E.A.; Hambach, U.; Gaudenyi, T.; Jovanović, M.; Stevens, T.; Zöller, L.; Machalett, B. Late Pleistocene loess-palaeosol sequences in the Vojvodina region, north Serbia. J. Quat. Sci. 2008, *23*, 73-84.

[72] Marković, S.B.; Stevens, T.; Kukla, G.J.; Hambach, U.; Fitzsimmons, K.E.; Gibbard, P.; Buggle, B.; Zech, M.; Guo, Z.T.; Hao, Q.Z.; Wu, H.; O'Hara-Dhand, K.; Smalley, I.J.; Ujvari, G.; Sümegi, P.; Timar-Gabor, A.; Veres, D.; Sirocko, F.; Vasiljević, Dj.A.; Jari, Z.; Svensson, A.; Jović, V.; Kovács, J.; Svirčev, Z. The Danube loess stratigraphy - new steps towards the development of a pan-European loess stratigraphic model. Earth Sci. Rev. 2015, 228-258.

[73] Popov, D.; Marković, S.B.; Jovanović, M.; Mesaroš Arsenović, D.; Stankov, U.; Gubik, D. Geomorphological investigations and GIS approach of the Tamiš loess plateau, Banat region (northern Serbia). Geographica Pannonica 2012b, *16*, 1-9.

[74] Jain, M.; Murray, A.S.; Bøtter-Jensen, L. Optically stimulated luminescence dating: how significant is incomplete light exposure in fluvial environments? Quatern. 2004, *15*, 143-157.

[75] Borsy, Z. Evolution of the alluvial fans of the Alföld. In: *Alluvial fans: a field approach*; Rachocki, A.H., Church, M., Eds.; Wiley and Sons Ltd.: Chichester, UK, 1990; 229-246.

[76] Berec B.; Gábris Gy. A Maros hordalékkúp bánsági szakasza (Alluvial fan of Maros River in Banat, Serbia–Romania). In: *Kárpát-medence: természet, társadalom, gazdaság (Carpathian Basin: nature, society, economy;* Frisnyák, S.; Gál, A., Eds.); Nyíregyháza–Szerencs, Hungary, 2013, pp. 51-64 (in Hungarian).

[77] Davis, B.A.S.; Passmore, D.G. Upper Tisza Project: radiocarbon analyses of Holocene alluvial and lacustrine sediments. Interim report on current analyses to the Excavation and Fieldwork committee 1998, *7*, University of Newcastle.

[78] Timar, G.; Sümegi, P.; Horvath, F. Late Quaternary dynamics of the Tisza River: evidence of climatic and tectonic controls. Tectonophysics 2005, *410*, 97-110.

[79] Kasse, C. Cold-climate aeolian sand-sheet formation in north-western Europe (c. 14-12.4 ka): a response to permafrost degradation and increased aridity. Permafrost and Periglacial Processes 1997, *8*, 295-311.

[80] Vandenberghe, J.; Kasse, C.; Bohncke, S.; Kozarski, S. Climate-related river activity at the Weichselian-Holocene transition: a comparative study of the Warta and Maas rivers. Terra Nova 1994, *6*, 476–485.

[81] Kasse, C.; Vandenberghe, J.; Bohncke, S. Climatic change and fluvial dynamics of the Maas during the Late Weichselian and Early Holocene. In *European river activity and climatic change during the Lateglacial and early Holocene*; Frenzel, B., Vandenberghe, J., Kasse, C., Bohncke, S., Gläser, B., Eds.; Paläoklimaforschung 1995, *14*, 123–150.

[82] Sidorchuk, A.; Borisova, O.; Panin, A. Fluvial response to the Late Valdai/Holocene environmental change on the East European Plain. Global Planet. Change 2001, *28*, 303-318.

[83] Sidorchuk, A.; Panin, A.; Borisova, O. Morphology of river channels and surface runoff in the Volga River basin (East European Plain) during the Late Glacial period. Geomorphology 2009, *113*, 137-157.

[84] Borisova, O.; Sidorchuk, A.; Panin, A. Palaeohydrology of the Seim River basin, Mid-Russian Upland, based on palaeochannel morphology and palynological data. Catena 2006, *66*, 53-73.

[85] Leopold, L.B.; Wolman, L.G.; Miller, J. Fluvial processes in Geomorphology; W.H. Freeman and co: San Francisco, USA, 1964; 522 pp.

[86] Petrovszki, J.; Timar, G.; Molnar, G. Is sinuosity a function of slope and bankfull discharge? - A case study of the meandering rivers in the Pannonian Basin. Hydrol. Earth Syst. Sci. Discuss. 2014, *11*, 12271-12290.

[87] Van Huissteden, J.; Vandenberghe, J. Changing fluvial style of periglacial lowland rivers during the Weichselian Pleniglacial in the eastern Netherlands. Zeitschr. f. Geomorphol., Suppl. Bd. 1988, *71*, 131-146.